HHS Public Access

Author manuscript

Biochemistry. Author manuscript; available in PMC 2017 September 20.

Published in final edited form as:

Biochemistry. 2016 September 20; 55(37): 5243–5255. doi:10.1021/acs.biochem.6b00446.

FABP1: A NOVEL HEPATIC ENDOCANNABINOID AND CANNABINOID BINDING PROTEIN

Huan Huang[†], **Avery L. McIntosh**[†], **Gregory G. Martin**[†], **Danilo Landrock**[‡], **Sarah Chung**[‡], **Kerstin K. Landrock**[‡], **Lawrence J. Dangott**[&], **Shengrong Li**[^], **Ann B. Kier**[‡], and **Friedhelm Schroeder**[†,*]

[†]Department of Physiology and Pharmacology, Texas A&M University, College Station, TX 77843

[‡]Department of Pathobiology, Texas A&M University, College Station, TX 77843

[&]Department of Biochemistry and Biophysics, Texas A&M University, College Station, TX 77843

[^]Department of Avanti Polar Lipids, 700 Industrial Park Dr., Alabaster, AL 35007-9105

Abstract

Endocannabinoids (EC) and cannabinoids are very lipophilic molecules requiring the presence of cytosolic binding proteins that chaperone these molecules to intracellular targets. While three different fatty acid binding proteins (FABP3, 5, 7) serve this function in brain, relatively little is known about how such hydrophobic EC and cannabinoids are transported within the liver. The most prominent hepatic FABP, liver fatty acid binding protein (FABP1, L-FABP), has high affinity for arachidonic acid (ARA) and ARA-CoA—suggesting that FABP1 may also bind ARA-derived ECs (AEA, 2-AG). Indeed, FABP1 bound EC with high affinity as shown by displacement of FABP1-bound fluorescent ligands and by quenching of FABP1 intrinsic tyrosine fluorescence. FABP1 also had high affinity for most non-ARA containing ECs, FABP1 inhibitors, EC uptake/hydrolysis inhibitors, phytocannabinoids, and less so synthetic cannabinoid receptor (CBR) agonists and antagonists. Physiological impact was examined with liver from wild-type (WT) versus FABP1 gene ablated (LKO) male mice. As shown by LC/MS, FABP1 gene ablation significantly increased hepatic levels of AEA, 2-AG, and 2-OG. These increases were not due to increased protein levels of EC synthetic enzymes (NAPEPLD, DAGL) or decreased level of EC degradative enzyme (FAAH), but correlated with complete loss of FABP1, decreased SCP2 (8-fold less prevalent than FABP1, but also binds ECs), and decreased degradative enzymes (NAAA, MAGL). These data indicated that FABP1 is not only the most prominent endocannabinoid and cannabinoid binding protein, but also impacts hepatic endocannabinoid levels.

Keywords

mouse; liver fatty acid binding protein; gene ablation; liver; endocannabinoid; cannabinoid

[*]Address Correspondence to: Friedhelm Schroeder, Department of Physiology and Pharmacology, Texas A&M University, 4466 TAMU, College Station, TX 77843-4466. Phone: (979) 862-1433, FAX: (979) 862-4929; fschroeder@cvm.tamu.edu.

INTRODUCTION

While brain receptors and enzymes comprising the endocannabinoid system (ECS) are increasingly understood, mechanisms whereby the highly hydrophobic endocannabinoids (EC) and cannabinoids are solubilized and traffic through brain cytosol to intracellular targets for metabolism have only recently been resolved (1–3). Pioneering work by Kaczocha, Deutsch, and colleagues demonstrated for the first time that three cytosolic fatty acid binding proteins found in brain (i.e. FABP3, FABP5, FABP7) all bind arachidonic acid (ARA)-derived EC (AEA, 2-AG) and cannabinoids (4–6). Importantly, pharmacological inhibition or ablation of these FABPs found in brain inhibits EC degradation, thereby enhancing EC accumulation and physiological action in brain (7–10). Surprisingly, although the liver form of fatty acid binding protein (FABP1) is not detectable in brain (11–13), nevertheless ablation of FABP1 markedly increases brain EC levels—especially AEA and 2-AG (13). The proposed mechanism whereby FABP1 gene ablation increases brain AEA and 2-AG levels is by its ability to bind ARA such that loss of FABP1 decreases hepatic ARA clearance, increases serum ARA availability for brain uptake, and increases brain ARA substrate for brain synthesis of AEA and 2-AG (13).

How FABP1 gene ablation may impact hepatic EC levels is not known and difficult to predict *a priori*. For example, FABP1 gene ablation inhibits uptake of other fatty acids by cultured primary hepatocytes and *in vivo* (14–16) while FABP1 overexpression enhances uptake of such fatty acids as well as ARA (17–20). This would suggest that FABP1 gene ablation would decrease hepatic ARA uptake and availability for synthesis of AEA and 2-AG, opposite to the increased AEA and 2-AG observed in brain of FABP1 gene ablated male mice (13). On the other hand, it may be postulated that FABP1 will also binds these ECs to enhance their cytosolic trafficking for enzymatic degradation—analogous to the impact of ablating/inhibiting FABPs found in brain (7–10). Since FABP1 has high affinity for ARA-CoA as well as ARA itself (21), we hypothesize that FABP1 may also bind other ARA-containing lipids (AEA, 2-AG), exogenous CB ligands (phytocannabinoids, synthetic cannabinoids), EC metabolic inhibitors, and impact hepatic AEA and 2-AG levels.

The work presented herein examined the possibility that FABP1 binds EC and cannabinoids through use of recombinant FABP1, quenching of intrinsic FABP1 tyrosine fluorescence, and displacement FABP1-bound fluorescent ligands by non-fluorescent EC, cannabinoids, and/or inhibitors. Functional significance of FABP1 in regulating hepatic EC levels and expression of proteins in the ECS was addressed in livers of wild-type (WT) versus FABP1 gene ablated (LKO) mice. The data showed that FABP1 has high affinity for ligands impacting the ECS. Furthermore, loss of FABP1 (LKO) elicited a sex-dependent increase in hepatic levels of AEA and 2-AG.

EXPERIMENTAL PROCEDURES

Materials

Cis-parinaroyl-CoA was synthesized from *cis*-parinaric acid, obtained from Invitrogen/Life Technologies (Grand Island, NY, USA), as described (22). NBD-AEA (NBD-N-arachidonoylethanolamide or [20-[(7-nitro-2-1,3-benzoxadiazol-4-yl)amino]

arachidonoylethanolamide) was synthesized by Dr. Shengrong Li and generously provided by Drs. Stephen Burgess and Walt Shaw (Avanti Polar Lipids, Alabaster, AL). NBD-stearic acid [12-N-methyl-(7-nitrobenz-2-oxa-1,3-diazo)aminostearic acid] was also obtained from Avanti Polar Lipids (Alabaster, AL). DAUDA (11-(dansylamino) undecanoic acid) was obtained from Cayman Chemical (Ann Arbor, MI). ANS (1-anilinonaphthalene-8-sulfonic acid) was from Life Technologies (Grand Island, NY). All reagents and solvents used were of the highest grade commercially available.

N-acylethanolamides and 2-monoacylglycerolss (2-MGs)

Unlabeled AEA (n-6 arachidonoylethanolamide), OEA (oleoylethanolamide), PEA (palmitoylethanolamide), DHEA (n-3 docosahexaenoylethanolamide), EPEA (n-3 eicosapentaenoylethanolamide), 2-AG (2-arachidonoylglycerol), 2-OG (2-oleoylglycerol), and 2-PG (2-palmitoylglycerol) were purchased from Cayman Chemical (Ann Arbor, MI). Deuterated AEA-d_4, OEA-d_2, PEA-d_4, DHEA-d_4, EPEA-d_4, and 2-AG-d_8 were also from Cayman Chemical (Ann Arbor, MI).

Phytocannabinoids, synthetic cannabinoids, and inhibitors

The native phytocannabinoids Δ^9-tetrahydrocannabinol (Δ^9-THC, also called dronabinol, psychoactive high affinity CB1 and CB2 agonist) and cannabidiol (non-psychoactive, very low affinity CB1 and CB2 indirect antagonist thought to attenuate the action of Δ^9-THC) were obtained from Cayman Chemical (Ann Arbor, MI). Synthetic cannabinoids obtained from Cayman Chemical (Ann Arbor, MI) were as follows: dronabinol (also called Δ^9-tetrahydrocannabinol or Δ^9-THC; high affinity CB1 and CB2 agonist), HU-210 (potent CB1 and CB2 receptor agonist analogue of Δ^9-THC), JWH 018 (high affinity CB1 and CB2 ligand, mildly selective for CB2); Rimonabant high affinity selective CB1 receptor inverse agonist), JWH-133 (high affinity, 200-fold selective CB2 agonist), SR-144528 (high affinity CB2 inverse agonist), CP55,940 (high affinity non-selective CBR agonist, more potent than Δ^9-THC). Synthetic cannabinoids that inhibit AEA uptake without affecting AEA hydrolysis (AM404), inhibit AEA uptake and weakly inhibit AEA hydrolysis (OMD1, OMD2), or inhibit AEA hydrolysis (VDM11) were purchased from Cayman Chemical (Ann Arbor, MI). BMS309403, known to bind/inhibit other FABPs (FABP3,4,5,7) was obtained from Cayman Chemical (Ann Arbor, MI). SCP2 inhibitors (SCPI1, SCPI3, and SCPI4) were from ChemBridge Corporation (San Diego, CA).

Recombinant proteins

Recombinant murine liver fatty acid binding protein (FABP1, L-FABP) (23), murine acyl CoA binding protein (ACBP) (24), and human sterol carrier protein-2 (SCP2) (25) were obtained as described in the cited papers from our laboratory.

Antibodies

Antibodies to liver proteins were obtained as follows: goat polyclonal anti-acyl-CoA-binding protein (ACBP, sc-23474), anti-fatty acid amide hydrolase (FAAH, sc-26427), anti-N-acylphosphatidylethanolamide phospholipase-D (NAPE-PLD; sc-163117), anti- fatty acid transport protein 4 (FATP-4; sc-5834), and liver-type fatty acid binding protein (FABP1, L-

FABP; sc-16064) from Santa Cruz Biotechnology (Santa Cruz, CA); rabbit polyclonal anti-monoacylglyceride lipase (MAGL, sc-134789); anti- diacylglycerol lipase α (DAGLα; sc-133307); mouse monoclonal anti-N-acylethanolamide-hydrolyzing acid amidase (NAAA; sc-100470) from Santa Cruz Biotechnology (Santa Cruz, CA); mouse polyclonal anti-fatty acid transport protein 5 (FATP5, ab89008); rabbit polyclonal anti fatty acid transport protein 2 (FATP2, ab83763) and specific monoclonal anti-mouse heat shock protein-70 (HSP70; ab2787) from Abcam (Cambridge, MA); mouse monoclonal glyceraldehyde 3-phosphate dehydrogenase (GAPDH, MAB374) from Millipore, Inc (Billerica, MA); rabbit polyclonal anti-sterol carrier protein-2 (recognizing 58 kDa SCPx, 15 kDa pro-SCP2, and 13.2 kDa SCP2) as described earlier (26).

Direct endocannabinoid binding to cytosolic 'chaperone' proteins (FABP1, SCP2, and ACBP): intrinsic tyrosine or tryptophan fluorescence

The major liver cytosolic lipidic ligand 'chaperone' proteins are each intrinsically-fluorescent due to the presence of Tyr or Trp residues as follows: Rat FABP1 has three Tyr residues but no Trp (27), SCP2 has a single Trp residue but no Tyr (25), and ACBP has four Tyr plus two Trp residues (28). Therefore, direct endocannabinoid binding to FABP1 was examined by quenching of intrinsic Tyr fluorescence as described earlier (29). Direct endocannabinoid (OEA) binding to SCP2 was determined similarly except that binding resulted in an increase in intrinsic Trp fluorescence emission when measured as in (25). Direct endocannabinoid binding to ACBP was determined similarly as for FABP1 as in (28).

Binding of N-acylethanolamides (NAEs), 2-monoacylglycerols (2-MGs), phytocannabinoids, synthetic cannabinoids, and inhibitors to cytosolic chaperone proteins (FABP1, SCP2, ACBP): displacement of protein-bound fluorescent ligands by non-fluorescent ligands

The following fluorescent ligand displacement assays at 24°C were used to further confirm and/or determine if the cytosolic lipidic ligand 'chaperone' proteins FABP1, SCP2, and ACBP also bound non-fluorescent NAEs, 2-MGs, phytocannabinoids, synthetic cannabinoids, or inhibitors: i) NBD-stearic acid displacement (26); ii) ANS displacement (29); iii) DAUDA displacement (30); iv) *cis*-parinaroyl-CoA displacement (25,31); and v) NBD-AEA displacement analogous to NBD-stearic acid displacement (26). Data were corrected for the following blanks/controls: protein only, fluorescent ligand only, fluorescent ligand with increasing amount of non-fluorescent ligand, and photobleaching. K_i values were calculated from the experimentally-obtained EC_{50} according to the equation EC50/[fluorescent ligand] = K_i/K_d using the known K_d values for: i) FABP1 binding NBD-stearic acid (K_d = 0.046 ± 0.008 μM), ANS (K_d = 2.5 ± 0.2μM), DAUDA (K_d = 0.464 ± 0.04 μM), and *cis*-parinaroyl-CoA (K_{d1}=27±4 nM, K_{d2}=66±8 nM) in the above cited papers; ii) FABP1 binding NBD-AEA (K_d = 0.70 ± 0.10 μM) and SCP2 binding NBD-stearate (K_d = 0.22 ± 0.03 μM) obtained similarly herein (not shown).

Animal care

Experimental protocols for animal use were approved by the Institutional Animal Care and Use Committee at Texas A&M University. Wild-type (WT) inbred male and female C57BL/6NCr mice 8 weeks were obtained, maintained, housed, and fed for an additional 4 weeks on

a phytol-free, phytoestrogen-free defined diet exactly as described earlier (13). Mice were fasted overnight, anesthetized (ketamine, 100 mg/kg; xylazine, 10 mg/kg), blood collected by cardiac puncture, and livers harvested for immediate flash freezing and storage at −80°C. Blood was processed to serum for storage at −80 °C. Mice were sentinel monitored quarterly and confirmed free of all known rodent pathogens.

N-Acylethanolamide (NAE) and 2-monoacylglycerol (2-MG) quantitation in liver

Following addition of deuterated internal standards, the NAEs and 2-MGs were extracted from liver homogenates as in (32) with modifications described in (13). The major N-acylethanolamides in liver (AEA, OEA, PEA, DHEA, and EPEA) were resolved and quantitated by liquid chromatography/mass spectrometry (LC/MS) in the Protein Chemistry Laboratory (directed by Dr. Larry Dangott at Texas A&M University) as in (33) modified as previously described (13). Individual 2-monoacylglycerols (2-AG, 2-OG, and 2-PG) were resolved and quantitated by LC/MS in the Protein Chemistry Laboratory (directed by Dr. Larry Dangott at Texas A&M University) also as described earlier (9,13).

QrtPCR to determine liver transcription of genes in the endocannabinoid system and other genes impacted by the endocannabinoid system

All procedures to extract total RNA, determine mRNA purity, and perform QrtPCR to determine mRNA levels of liver genes were performed analogous to those for brain as described earlier (13). The following hepatic mRNA levels were determined: N-acylphosphatidylethanolamide phospholipase-D (*Napepld*, Mm00724596_m1); diacylglycerol lipase α (*Dagla*, Mm00813830_m1); diacylglycerol lipase β (*Daglb*, (Mm00523381_m1); fatty acid amide hydrolase (*Faah*, Mm00515684_m1); N-acylethanolamide-hydrolyzing acid amidase (*Naaa*, Mm01341699_m1); 2-monoacylglycerol lipase (*Mgll*, Mm00449274_m1); cannabinoid receptor-1 (*Cnr1*, Mm01212171_s1); cannabinoid receptor-2 (*Cnr2*, Mm02620087_s1); transient receptor potential cation channel subfamily V member 1 (*Trvp-1*, Mm01246302_m1), Peroxisome Proliferator-Activated Receptor Alpha (*Ppara*, Mm00440939_m1); Peroxisome Proliferator-Activated Receptor Beta/Delta (*Ppard,* Mm00803184_m1); Carnitine Palmitoyltransferase 1A (*Cpt1a*, Mm00550438_m1); Acyl-CoA Oxidase 1 (*Acox1*, Mm00443579_m1); Sterol Regulatory Element Binding Transcription Factor 1 (*Srebf1*, Mm01138344_m1); Acetyl-CoA Carboxylase Alpha (*Acaca*, Mm01304285_m1); Fatty Acid Synthase (*Fasn* Mm00662319_m1); Adipose Triglyceride Lipase (*Pnpla2*, Mm00503040_m1); CGI58 (*Abhd5*, Mm00470734_m1). Each sample reaction (10μL total volume each) was performed in duplicate in 96 well optical reaction plates (Applied Biosystems®, Foster City, CA). The mRNA data were normalized to the 18S RNA housekeeping gene. For final calculations, the data were made relative to the control mouse group (male WT mice on control diet).

Western blotting to determine liver protein translation products for enzymes and Ooher proteins in the endocannabinoid system

Liver post nuclear supernatants (PNS) were subjected to sodium dodecyl sulfate–polyacrylamide gel electrophoresis (SDS-PAGE) to resolve proteins for detection and quantitation by western blot analysis similarly as described earlier for brain (13). Western blotting was performed to determine relative protein levels of: acyl CoA binding protein

(ACBP), cannabinoid receptor-1 (CB1), diacylglycerol lipase A (DAGL-A), fatty acid amide hydrolase (FAAH), fatty acid binding protein-1 (FABP1), fatty acid transport protein 2 (FATP-2), fatty acid transport protein 4 (FATP-4), fatty acid transport protein 5 (FATP5), heat shock protein-70 (HSP70), 2-monoacylglycerol lipase (MAGL), N-acylethanolamide-hydrolyzing acid amidase (NAAA), N-acylphosphatidylethanolamide phospholipase-D (NAPE-PLD), and sterol carrier protein 2 (recognizing 58 kDa SCPx, 15 kDa pro-SCP2, and 13.2 kDa SCP2). GAPDH, β-Actin or COX-4 was used as internal loading control. Densitometric analysis was performed using ImageJ software (National Institutes of Health, Bethesda, MD) to quantify individual protein bands for normalization to loading control as in (13). Representative cropped western blots were inserted into figure panels similarly as in earlier publications where individual blots were separated by a white line/space.

Statistical analysis

Values are the mean ± standard error of the mean (SEM). One-way analysis of variance (ANOVA), followed with the Newman-Keuls post-hoc analysis either with GraphPad software (La Jolla, CA) or Sigma Plot software (Systat, San Jose, CA), was used for all statistical analyses. P-values of $p < 0.05$ were considered statistically significant and denoted by a * (FABP1 KO vs wild-type) or # (Male vs Female of the same genotype) in the tables or figure panels.

RESULTS

Direct binding of endocannabinoids to FABP1

FABP1 exhibits high affinity for arachidonic acid (ARA, C20:4n-6) and its CoA thioester (20,21,34). However, it is not known if FABP1 also binds the ARA-containing endocannabinoids AEA or 2-AG. To begin to address this issue, direct AEA binding to FABP1 was measured by determining its impact on FABP1 intrinsic aromatic amino acid (Tyr) fluorescence. AEA decreased FABP1's intrinsic Tyr fluorescence emission intensity at 304 nm (Fig. 1A) analogous to that shown by other FABP1 ligands such as oleic acid and oleoyl-CoA (27).

Binding of N-acylethanolamides (NAEs) to FABP1: displacement of protein-bound fluorescent ligands by non-fluorescent ligands

To further establish the ability of FABP1 to bind NAEs, displacement of FABP1-bound fluorescent ligands by native non-fluorescent AEA and other N-acylethanolamides was determined.

Since FABP1 binds NBD-stearic acid (26,29) and AEA as well as cannabinoids displace NBD-stearic bound by the three major brain FABPs, i.e. FABPs 3, 5, 7 (4,6), the possibility that AEA would similarly displace FABP1-bound NBD-stearic acid was examined. However, AEA did not displace FABP1-bound NBD-stearic acid (not shown). Likewise, although FABP1-bound ANS is displaced by many other FABP1 ligands (fatty acids, fibrates, phthalates, and others) (29,35,36), AEA did not displace FABP1-bound ANS (not shown). Even FABP1-bound DAUDA, which is displaced by other lipidic ligands (30), was only very weakly (13%) displaced by very high AEA concentration (e.g. 9 μM) (not shown).

These data suggested that the ethanolamide group of AEA may significantly impact the localization of AEA's arachidonoyl group within the FABP1 binding site as compared to the localization of FABP1-bound unesterified fatty acid probes (NBD-stearic acid, DAUDA) or even ANS which binds to the FABP1 protein polypeptide chain.

This possibility was addressed using a *cis*-parinaroyl-CoA displacement assay developed by our laboratory (22,25). The *cis*-parinaroyl-CoA displacement assay has two key advantages over the above assays: i) Analogous to the carboxyl of ARA being esterified to the polar ethanolamide moiety in AEA, the carboxyl of *cis*-parinaric acid is esterified to a polar CoA group in *cis*-parinaroyl-CoA (21); ii) Since FABP1 has two *cis*-parinaroyl-CoA binding sites (21), this allowed determination of whether AEA displaced only one or both of the FABP1-bound *cis*-parinaroyl-CoAs. Representative *cis*-parinaroyl-CoA displacement curves showed that AEA maximally displaced about 50% of FABP1-bound *cis*-parinaroyl-CoA (Fig 2A). Analysis of multiple FABP1-bound *cis*-parinaroyl-CoA displacement curves showed that FABP1 bound AEA with high affinity, K_i=0.111±0.003 μM (Table 1).

Likewise, FABP1 bound almost all other N-acylethanolamides (NAE) tested. Each of the unsaturated NAEs tested (OEA, EPEA, DHEA) displaced FABP1-bound *cis*-parinaroyl-CoA (Fig. 2B,C). Analysis of multiple FABP1-bound *cis*-parinaroyl-CoA displacement curves showed that FABP1 bound the monounsaturated oleic acid-containing ethanolamide (OEA) with highest affinity, K_i=0.043±0.004μM (Table 1). The n-3 polyunsaturated fatty acid containing ethanolamides, i.e. eicosapentaenoylethanolamide (EPEA) and docosahexaenoylethanolamide (DHEA), were also bound but 4–10 fold more weakly as shown by K_is of 0.39±0.03 and 0.163±0.004 μM, respectively (Table 1). In contrast, the saturated palmitic acid-containing PEA did not displace either FABP1-bound *cis*-parinaroyl-CoA or FABP1-bound NBD-AEA (Table 1). Taken together, the FABP1-bound *cis*-parinaroyl-CoA and/or NBD-AEA displacement assays established that FABP1 had a single binding site for AEA and unsaturated NAEs with affinities in the overall order: OEA > AEA > EPEA, DHEA ⋙ PEA.

Binding of native 2-monoacylglycerides (2-MGs) to FABP1: displacement of FABP1-bound fluorescent cis-parinaroyl-CoA by non-fluorescent ligands

To determine if FABP1 also binds 2-MGs, the *cis*-parinaroyl-CoA displacement assay was applied as described in Methods.

Not only 2-AG, but 2-monoacylglycerols (2-MGs) such as 2-oleoylglycerol (2-OG) and 2-palmitoylglycerol (2-PG) displaced FABP1-bound *cis*-parinaroyl-CoA. 2-AG maximally displaced about 50% of FABP1-bound *cis*-parinaroyl-CoA (Fig 3)—consistent with a single site as shown for direct AEA binding above. Likewise, the monounsaturated fatty acid containing 2-OG displaced FABP1-bound *cis*-parinaroyl-CoA to almost similar extent (Fig. 3). Interestingly, unlike the saturated palmitic acid containing PEA (Table 1), the palmitic acid-containing 2-PG displaced FABP1-bound *cis*-parinaroyl-CoA—albeit not as effectively as 2-AG or 2-OG (Fig 3). Analysis of multiple FABP1-bound *cis*-parinaroyl-CoA displacement curves showed that FABP1 bound native non-fluorescent 2-AG with high affinity, K_i=0.061±0.001 μM (Table 1). FABP1 also bound 2-OG and 2-PG with high

affinity as demonstrated by K_is of 0.040±0.003 μM and 0.070±0.005 μM, respectively (Table 1).

In summary, FABP1 bound polyunsaturated fatty acid containing 2-AG, monounsaturated fatty acid containing 2-OG, and saturated fatty acid containing 2-PG in the overall order: 2-OG > 2-AG, 2-PG. This suggested potential roles for FABP1 in reuptake and intracellular targeting/degradation of 2-MGs as well as NAEs.

Binding of inhibitors to FABP1: displacement of FABP1-bound fluorescent cis-parinaroyl-CoA by non-fluorescent inhibitors

While BMS309403 is a synthetic molecule shown to bind and inhibit a variety of FABPs including FABP4 (37) as well as FABPs 3,5, and 7 (6,9), it is not known if FABP1 also binds BMS309403 and/or possibly other inhibitors employed to manipulate the endocannabinoid system. This possibility was examined using the FABP1-bound *cis*-parinaroyl-CoA displacement described in Methods.

BMS309403 maximally displaced FABP1-bound *cis*-parinaroyl-CoA almost completely (Fig 4B)—consistent with BMS309403 displacing *cis*-parinaroyl-CoA from both of binding sites within FABP1 (21). Analysis of multiple displacement curves demonstrated that FABP1 has high affinity for BMS309403 as shown by K_{i1}=0.021±0.001μM, K_{d2}=0.052±0.001μM (Table 1).

Although cellular uptake fatty acids across the plasma membrane appears to be mediated by both protein-mediated as well as diffusional mechanisms (38–41), the available evidence indicates that endocannabinoid uptake across the plasma membrane is primarily diffusional (3,42). Since inhibitors such as AM404, OMDM-1, and OMDM-2 are thought to inhibit AEA uptake, the possibility that they might do so by binding to cytosolic chaperones such as FABP1 was examined. AM404, OMDM-1, and OMDM-2 all displaced FABP1-bound *cis*-parinaroyl-CoA, the maximal extent of displacement approaching about 50% (Fig 4A). Likewise, an inhibitor of AEA hydrolysis (VDM11) also maximally displaced about 50% of FABP1-bound *cis*-parinaroyl-CoA (Fig 4A). Analysis of multiple displacement curves showed that all of these inhibitors of AEA uptake (AM404, OMDM-1, OMDM-2) or hydrolysis (VDM11) were bound with very similar high affinity by FABP1 as shown by K_is of 0.04 μM (Table 1).

FABP1 binding of compounds (SCPI1, SCPI3, and SCPI4) that inhibit another potential cytosolic endocannabinoid chaperone, i.e. SCP2 (see following sections), was examined with NBD-stearate and ANS displacement assays. NBD-stearate and ANS were used because of SCPI's high absorbance in the region of *cis*-parinaroyl-CoA's emission. SCPI1 displaced FABP1 bound NBD-stearate (Fig. 4C, closed dark circles. K_i = 0.35 ± 0.05μM, Table 1), but not ANS (Fig. 4D, closed dark circles). In contrast, SCPI4 displaced FABP1 bound ANS (Fig. 4D, black triangles. K_i=0.033 ± 0.002μM, Table 1), but only displaced about 20% FABP1 bound NBD-stearate (Fig. 4C, black triangles). SCPI3 displaced NBD-stearate more weakly (K_i = 0.9 ± 0.1μM, Table 1).

In summary, FABP1 bound the general FABP binding inhibitor BMS309403 at both fatty acyl-CoA binding sites. In contrast, FABP1 bound the inhibitors of AEA uptake/hydrolysis at a single site similar to FABP1 binding only a single NAE or 2-MG. Interestingly, FABP1 also bound inhibitors (SCPI1, SCPI3, SCPI4) of SCP2, another potential endocannabinoid chaperone.

Binding of phytocannabinoids and synthetic cannabinoids to FABP1: displacement of FABP1-bound fluorescent cis-parinaroyl-CoA and/or NBD-AEA by non-fluorescent ligands

Since both endocannabinoids (AEA, 2-AG) and cannabinoids bind to CB1 receptors (43), the possibility that FABP1 also binds cannabinoids was considered and tested in the *cis*-parinaroyl-CoA and NBD-AEA displacement assays.

The phytocannabinoids (THC, cannabidiol) differentially impacted FABP1 bound *cis*-parinaroyl-CoA. THC maximally displaced essentially all of FABP1-bound NBD-AEA from its single binding site (Fig. 5A, open circles). Likewise, THC maximal displacement of FABP1 bound *cis*-parinaroyl-CoA approached 50% (Fig. 6A)—again consistent with displacing *cis*-parinaroyl-CoA from only one of FABP1's two binding sites for *cis*-parinaroyl-CoA (21). Analysis of multiple displacement curves indicated that THC displaced FABP1-bound NBD-AEA with K_i = 1.0±0.2 μM (Table 2). Cannabidiol maximally displaced about 50% of FABP1-bound *cis*-parinaroyl-CoA (Fig 5B). Analysis of multiple displacement curves yielded a K_i = 0.167±0.009 μM for cannabidiol (Table 2).

With regards to the synthetic cannabinoids, most much more weakly (Fig. 5C and 5D) or did not displace FABP1-bound *cis*-parinaroyl-CoA or bound NBD-AEA (Fig. 5E), except JWH018. One synthetic cannabinoid SR144528 actually increased the fluorescence of FABP1-bound NBD-AEA but not bound *cis*-parinaroyl-CoA (Fig 5E). Analysis of multiple displacement curves showed that the synthetic CB1 receptor agonists HU-210 displaced FABP1-bound NBD-AEA with K_i=0.85, while the full CB1 and CB2 receptor agonist JWH-018 displaced FABP1-bound *cis*-parinaroyl-CoA with K_i=0.058±0.005 (Table 2). The selective central CB1 receptor inverse agonist rimonabant displaced FABP1-bound NBD-AEA with K_i=2.0±0.4 μM (Table 2). The synthetic cannabinoids that are more selective for peripheral CB2 receptor (JWH-133, SR-144528) did not displace either FABP1-bound NBD-AEA or bound *cis*-parinaroyl-CoA (Table 2). The THC mimic CP55,940 more weakly displaced FABP1-bound *cis*-parinaroyl-CoA with K_i=0.99±0.07μM (Table 2).

Taken together, these data showed that FABP1 bound phytocannabinoids and synthetic cannabinoids, especially those bound to CB1 receptors, but much less or not those that were CB2 receptor selective. This suggested potential roles for FABP1 in hepatic uptake and intracellular targeting/degradation of phytocannabinoids and their synthetic agonist and antagonist analogues.

FABP1's Specificity as a Potential Cytosolic NAE and 2-MG 'Chaperone': Intrinsic Tryptophan and Tyrosine Fluorescence of SCP2 and ACBP

To establish specificity of EC binding to FABP1, the possibility that that these EC are also bound by other liver cytosolic 'chaperones' of lipidic ligands was examined. SCP2 and ACBP share in common with FABP1 the ability to bind fatty acyl CoAs (25), while SCP2

and FABP1 both also bind fatty acids (21,44). Therefore, the impact of EC binding on intrinsic Trp and Tyr emission of SCP2 (contains 1 Trp, no Tyr) and ACBP (contains 3 Tyr, no Trp) was determined as described in Methods.

With regards to SCP2, OEA significantly increased SCP2's maximal fluorescence emission of Trp near 335 nm (Fig. 1B), analogous to the effect of oleoyl-CoA binding on SCP2 Trp fluorescence emission (25). With increasing OEA, SCP2 Trp fluorescence emission increased to a plateau typical of a saturation binding curve (Fig. 1C). Analysis as described in Methods yielded a K_d of 0.39 μM for SCP2 binding OEA. Inhibitors of SCP2 such as SCPI1, SCPI3, and SCPI4 as well as the FABP inhibitor BMS309403 displaced SCP2-bound NBD-stearic acid (Fig. 1D), with K_is of 0.68±0.06 μM, 3.9±0.1 μM, 2.9±0.2μM, and 5.5 ± 0.5μM for SCPI1, SCPI3, SCPI4, and BMS309403, respectively.

Finally, neither OEA nor AEA quenched ACBP aromatic amino acid fluorescence emission of ACBP Tyr (Fig 1F). This was in marked contrast to the impact of another known ACBP ligand (oleoyl-CoA) which significantly quenched the intrinsic Tyr fluorescence emission of ACBP (Fig. 1E), consistent with earlier studies (28),

Taken together, SCP2 (but not ACBP) also directly bound EC as well as known inhibitors of SCP2 and FABPs. This suggested SCP2 as another EC 'chaperone' protein in the cytosol and potentially a pharmaceutical target.

FABP1 ablation (LKO) elicits sex-dependent increase liver levels of endocannabinoid AEA and differentially impacts other NAEs

FABP1 has high affinity for arachidonic acid (ARA, C20:4n-6) which is the precursor of ARA-derived AEA (20,21,45). However, as shown herein FABP1 also has high affinity for AEA itself which may chaperone AEA and 2-AG to intracellular enzymes for degradation. To determine the physiological net effect of these opposite influences on AEA level, LC/MS was used to quantitate hepatic AEA and other NAEs in livers of wild-type (WT) and FABP1 gene ablated (LKO) mice. While all the major NAEs were qualitatively present in livers of both WT and LKO mice, quantitative amounts were highly dependent on FABP1 gene expression in a sexually dimorphic manner.

Livers of male wild-type (WT) mice had low levels of n-3 polyunsaturated LCFA containing NAEs, i.e. AEA (Fig. 6A), DHEA (Fig 6D) or EPEA (Fig 6E), and relatively higher levels of OEA (Fig. 6B) and PEA (Fig. 6C). LKO increased hepatic levels of AEA (Fig 6A) and EPEA (but not DHEA, Fig. 6D,E), decreased or trended to decrease levels of OEA and PEA (Fig 6B,C) in livers of male mice.

In contrast, livers of WT female mice had at least 7-fold lower levels of AEA (Fig 6A) and EPEA (Fig 6E) concomitant with higher levels of PEA (Fig 6C) and DHEA (Fig 6D) as compared to their WT male counterparts. In female mice, LKO did not alter liver levels of AEA, OEA, or EPEA (Fig 6A,B,E), but instead markedly increased that of PEA (Fig 6C) while decreasing that of DHEA (Fig 6D).

Taken together, the data showed that WT females had much lower level of the endogenous CB receptor agonist AEA, compensated for only in part by higher PEA levels. The much

lower level of EPEA in WT females was compensated by much higher level of DHEA. Finally, LKO selectively increased the hepatic level of AEA only in males, while increasing that of PEA in females.

FABP1 ablation (LKO) elicits sex-dependent increase in liver endocannabinoid 2-AG and 2-OG

LC/MS resolved and quantitated all three major 2-MGs in liver, with the respective levels again highly dependent on FABP1 gene expression in a sexually dimorphic manner.

Wild-type (WT) male mouse livers had at least 10-fold higher levels of the other endogenous CB1 receptor agonist 2-AG (Fig 6F) as compared to that of AEA (Fig 6A). WT male liver level of 2-OG (Fig 6G) was nearly 8-fold higher than that of 2-AG (Fig 6F) while the level of 2-PG (Fig 6H) was similar to that of 2-AG (Fig 6F). LKO significantly increased hepatic levels of 2-AG (Fig 6F) and 2-OG (Fig 6G), but not 2-PG (Fig 6H) in males.

Livers of female mice had much higher levels of the endogenous CB receptor agonist 2-AG (Fig 6F) and 2-OG (Fig 6G), but not 2-PG (Fig 6H), as compared to WT males. FABP1 gene ablation did not further impact the level of 2-AG (Fig 6F) and actually decreased that of 2-OG (Fig 6G) in livers of female mice. Thus, livers of both WT (and even more so LKO) mice had markedly higher levels of the CB agonist 2-AG as compared to the other CB agonist AEA. Further, WT females had higher levels of 2-AG and 2-OG as compared to males. LKO selectively increased 2-AG and 2-OG levels in livers of males, but not females.

Impact of FABP1 ablation (LKO) on liver protein levels of enzymes in endocannabinoid synthesis and degradation

Almost nothing is known about the impact of sex on protein levels of liver enzymes in endocannabinoid synthesis or degradation. Western blotting showed that NAPE-PLD was not significantly different between WT males and females (Fig. 7A), but that of DAGLα was lower in WT females compared to males (Fig. 7B). Although LKO did not alter NAPEPLD in either sex (Fig. 7A), DAGLα was decreased by LKO mice in both sexes (Fig. 7B).

With regards to enzymes for endocannabinoid degradation/hydrolysis (FAAH, NAAA), western blotting showed that FAAH was significantly higher in the females vs. males (Fig. 7C) and NAAA was lower in females (Fig. 7D) while MAGL did not differ (Fig 7E). LKO had no impact of FAAH in either sex (Fig. 7C), decreased NAAA in males (Fig. 7D), and decreased MAGL in both sexes (Fig. 7E).

Overall, these data indicated that the higher levels of AEA and 2-AG (along with higher potentiating ‘entourage’ 2-OG) in livers of male FABP1 gene ablated mice were not associated with increased protein levels of the respective endocannabinoid synthetic enzymes (NAPEPLD, DAGLα). While the higher AEA level in LKO males was not associated with any decreased protein level of the major AEA degradative/hydrolytic enzyme FAAH, it was associated in part to decreased level of the less prevalent NAAA. In contrast, higher 2-AG in LKO males was associated with decreased protein level of 2-AG degradative/hydrolytic enzyme MAGL.

Effect of FABP1 gene ablation (LKO) on liver protein levels of membrane transport/translocase proteins involved in arachidonic acid (ARA) uptake

Three membrane associated proteins (FATP2, FATP4 and FATP5) facilitate translocation/uptake of long chain fatty acids such ARA in liver (46). Western blotting of liver homogenates from WT male and female mice showed that males did not differ from females in liver level of FATP2 (Fig 8B), but females had higher protein levels of FATP4 and FATP5 (Fig 8A,C). LKO had no impact on any of these membrane fatty acid translocase/transport proteins localized in either the plasma membrane FATP5 (Fig 8A) or in intracellular membranes, FATP2 or FATP4 (Fig. 8B,C).

These data indicate that the overall higher level of total ARA-containing ECs (AEA + 2-AG) in female livers as compared to males was associated at least in part with higher protein levels of membrane fatty acid transporters/translocases involved in hepatic ARA uptake. In contrast, the FABP1 gene ablation-induced increase in liver AEA and 2-AG levels in males was not associated with higher expression of membrane proteins involved in ARA uptake. LKO did not further affect liver levels of these proteins in females.

Impact of FABP1 gene ablation (LKO) on liver protein levels of cytosolic ARA, AEA, and 2-AG ‘chaperone’ proteins

Liver expresses at least three cytosolic proteins involved in the uptake and intracellular chaperoning of fatty acids such as ARA and their CoA thioesters: FABP1 (21), sterol carrier protein-2 (SCP2) (25), and ACBP (28). Two of these (FABP1, SCP2), but not ACBP, also bind and potentially chaperone endocannabinoids (e.g. AEA, 2-AG) to/from sites of synthesis and degradation (Table 1, Figs. 1–3). In addition, liver also expresses one other known endocannabinoid binding/chaperone protein, i.e. HSP70 (47). Therefore, quantitative western blotting was performed as described in Methods to determine the impact of sex and FABP1 gene ablation on these hepatic proteins.

Liver cytosolic ‘chaperone’ levels were differentially expressed in males vs females. On a ng/μg liver protein basis, hepatic levels of FABP1 (Fig. 8D) and SCP2 (Fig. 8E) were lower in females than males. In contrast, liver protein levels of ACBP and HSP70 did not differ between the sexes (Fig. 8F,G). Consequently, the quantitative pattern of chaperone expression in males (FABP1, HSP70, ACBP > SCP2) differed somewhat from that in females (ACBP > FABP1, HSP70 > SCP2).

LKO resulted in complete loss of FABP protein in both males and females as expected (Fig. 8D). Loss of FABP1 was not compensated for by concomitant upregulation of SCP2, ACBP, or HSP70 in either males or females (Fig. 8E,F,G). Instead, hepatic protein levels of SCP2 were significantly decreased (Fig. 8E) in male LKO livers. In contrast, hepatic protein levels of SCP2, ACBP, and HSP70 were not significantly altered by FABP1 gene ablation (Fig. 8E–G) in female mice.

Taken together, these data showed that on a protein mass basis the livers of male WT mice expressed much higher levels of EC binding proteins (FABP1, HSP70 > SCP2) as compared to females. This in turn correlated with male livers having lower basal levels of total ARA-containing ECs (AEA + 2-AG) as well as non-ARA-containing ECs (2-OG, PEA) (Fig. 6).

By analogy, reduction of cytosolic EC chaperones in brain is known to reduce EC degradation/hydrolysis to thereby raise brain EC levels (7–9). Since LKO decreased (males) or did not alter (females) protein levels of other hepatic EC chaperone proteins, the total loss of cytosolic EC binding/chaperone capacity was much greater in livers of male than female LKO mice. This in turn correlated with marked upregulation of ECs (AEA, 2-AG) and potentiating non-ARA containing NAEs and 2-MGs (Fig. 6) in males, but not females.

Effect of FABP1 gene ablation (LKO) on liver protein level of the major cannabinoid receptor, CB1

While present at lower levels than in brain, nevertheless liver expresses the endocannabinoid receptor CB1 (hepatocytes), but only very low level of CB2 (Kuppfer cells) (1,48). Our studies showed that livers of male LKO mice had significantly reduced protein levels of CB1 (Fig. 7F) in comparison to male WT mice. In contrast, the LKO female mice had significantly increased CB1 protein levels (Fig. 7F) in comparison to both male and female WT livers. Thus, the lower LKO male liver level of CB1, the major ARA and 2-AG receptor in liver, inversely correlated with the male LKO liver's higher level of total ARA-containing ECs (AEA + 2-AG) (Fig. 6). Although the CB1 level was significantly increased in the female LKO mice in comparison to the female WT mice, the total ARA-containing ECs (AEA + 2-AG) were unchanged.

FABP1 ablation (LKO) elicits selective sex-dependent alteration in expression of liver receptors and proteins involved in fat accumulation

Endocannabinoid (AEA, 2-AG) activation of CB1 receptors facilitates fat accumulation in liver through activation of SREBP1, while other NAEs induce PPARα (1,48,49).

While livers of male and female mice did not or only slightly differed in transcription of mRNAs for *Ppara*, *Pparb*, or *Srebpf1* (Table 3), transcription of liver PPARα-regulated genes in fatty acid oxidation (*Cpt1A*, *Acox1*) was higher in males (Table 3). Conversely, transcription of SREBP1 target gene mRNAs (*Acaca, Fasn*) encoding proteins in *de novo* fatty acid synthesis did not differ between the sexes (Table 3). Transcription of the triacylglyceride hydrolytic enzyme (*Pnpla2*) also did not differ between the sexes, but that of its positive regulator (*Abhd5*) was significantly lower in males (Table 3). LKO selectively increased mRNA levels of these three nuclear receptors in livers of females (but not males) in the order *Srebpf1* ⋙ *Ppara* > unaltered *Pparb* (Table 3). Nevertheless, LKO increased transcription of SREBP1c target gene (*Fasn*) in both males and females (Table 3). LKO did not alter transcription of *Abhd5* or *Pnpla2* in males, but significantly increased that of *Pnpla2* in females (Table 3). Taken together, these findings suggested that LKO impacted mRNA levels of liver nuclear receptors and target genes in a complex manner only partially attributed to changes in mRNA levels of affected genes.

DISCUSSION

Because of their very lipophilic nature, endocannabinoids are highly membrane-associated and require soluble 'chaperone' proteins to facilitate their solubilization and cytosolic trafficking for targeting to intracellular organelles and degradation/hydrolysis (1,3). Ground-

breaking discoveries by Kaczocha, Deutsch, and colleagues for the first time demonstrated that brain cytosol contains three fatty acid binding proteins (FABP3, FABP5, FABP7) that bind both ARA-derived ECs (AEA, 2-AG) and cannabinoids to facilitate their intracellular targeting for degradation (4–6). While the liver also has a functional endocannabinoid system (50,51), relatively little is known regarding the identity of the corresponding EC 'chaperone(s)' in liver cytosol. While relatively large (70 kDa) liver protein HSP70 has heretofore been shown to bind AEA, its affinity was very weak as evidenced by K_d = 3.7 ± 0.5 μM (47). However, liver does contain three families of 10–14 kDa soluble proteins (FABP1, ACBP ≫ SCP2) that analogously bind and 'chaperone' a variety of other lipidic ligands through hepatic cytosol (52). The finding that these proteins exhibit high affinity for arachidonoyl-CoA (ARA-CoA) (21,22,25), suggested that they might also bind ARA esterified to other molecules such as ethanolamide and glycerol, i.e. the ARA-derived ECs (AEA, 2-AG). This possibility was examined with the respective recombinant proteins, fluorescent endocannabinoid binding assays, and livers of FABP1 gene ablated mice. The results contributed several key new insights to our understanding of the hepatic endocannabinoid system:

First, FABP1 and SCP2, but not ACBP, bind endocannabinoids (EC) with high affinity. FABP1 bound AEA and 2-AG ≥3-fold more strongly as compared to SCP2 (13). In fact, FABP1 bound AEA and 2-AG with the highest affinity yet reported for any FABP family member. For example, FABP1 bound AEA 8–10-fold more strongly as compared to FABP3, FABP5, and FABP7 (4). Similarly, FABP1 bound 2-AG with 2–15-fold stronger affinity versus FABP3, FABP5, and FABP7 (4). A caveat, however, is that FABP1 binding determined herein and earlier for SCP2 (13) was determined by displacement of bound *cis*-parinaroyl-CoA while that of FABP3,5, and 7 was by displacement of NBD-stearic acid, a ligand not displaced from FABP1 by AEA (shown herein). Since different binding assays may give rise to somewhat different affinities for the same ligand, it would be of interest in future studies to determine FABP3, 5, and 7's affinities for AEA using the *cis*-parinaroyl-CoA displacement assay. It is important to note, however, that FABP1 is not detected in brain (11,12,53), while the FABP3,5 and 7 found in brain are not present or only at very low level in liver (52). Taken together, these data indicated FABP1 as the first non-CNS FABP capable of binding ECs.

Second, FABP1 also bound both phytocannabinoids and synthetic cannabinoids. FABP1's affinities for THC and several synthetic cannabinoids (HU-210, rimonabant, CP55,940) were in the same range as that shown by FABP3, FABP5, and FABP7 for THC (4). Interestingly, FABP1 bound cannabidiol and synthetic cannabinoids such as JWH018 with even higher affinities (0.05 to 0.16 μM) which were 9–11 fold stronger than exhibited by FABP3,5, and 7 for cannabidiol (4). Taken together with the fact that the FABPs present in brain are not or only weakly very detectable in liver (52), these data indicated FABP1 as the first known hepatic cytosolic chaperone protein for cannabinoids.

Third, FABP1 bound a variety of inhibitors of the EC system as well as inhibitors of SCP2. FABP1 had very high affinity (29–40 nM Ki range) for synthetic inhibitors of AEA uptake —as much as 130-fold more strong binding than that exhibited by FABP5 found in brain (6). Likewise, FABP1 had even higher affinity for the FABP inhibitor BMS309403 (Ki up to

21nM). In contrast, FABP1 bound BMS309403 much more strongly than FABPs found in brain: 12–50-fold more strongly than FABP5; 10-fold more strongly than FABP3 (4,6). Only the adipocyte FABP4 bound BMS309403 with higher affinity (<2 nM) than FABP1 (20 nM) (37). These data suggest a preliminary order of relative BMS309403 affinities (FABP4 > FABP1 ≫ FABP3, FABP5). However, this order may be subject to change since the reported studies determined Kis using displacement of different ligands (cis-parinaroyl-CoA, ANS, NBD-stearic acid). While analogous high affinity inhibitors (SBF126, SBF150, SBF160, SBF162) with specificity for FABP7, but not FABP3 or 5, have been reported (9), their specificity for FABP1 is not known. Finally, FABP1 also bound inhibitors of SCP2 with a wide range of affinities, some as high as that for AEA (SCPI4) and others similar to those for THC, cannabidiol, and some synthetic cannabinoids (SCPI1, SCPI3). Taken together, these data suggested FABP1 as a novel extra-CNS therapeutic target for chemical inhibitors of EC binding, transport, and metabolism.

Fourth, FABP1 is the most prevalent cytosolic protein capable of binding EC, cannabinoids, and inhibitors of the endocannabinoid system. Quantitative western blotting showed that the hepatic FABP1 concentration was nearly 10-fold higher than that of SCP2—consistent with earlier studies (38,52,54,55). Moreover, nearly half of hepatic SCP2 is sequestered in the peroxisomal matrix rather than cytosol (56). Importantly, ACBP did not bind EC, as shown herein. Although quantitative Western blotting showed that, despite being present at equal mass as FABP1 in liver (Fig. 8), the molar amount of HSP70 was actually 5-fold lower than that of FABP1 due to HSP70's much greater molecular weight. Despite the high prevalence of FABP1 in hepatic cytosol (0.1–1.0mM or 2–10% of soluble protein) (29,38,52,57), FABP1 has enough unoccupied binding sites (25% of total) that are more than sufficient to accommodate binding of ECs (58–60). Finally, it is important to note that FABP1 concentration in liver cytosol (29,38,52,57) is >10-fold higher than the sum of FABP3, 5, and 7 in brain (61–63). This would suggest that hepatic FABP1 may effectively compete with and regulate availability of cannabinoids, CB receptor agonists/antagonists, and/or inhibitors brain for uptake/metabolism by brain. Consistent with this possibility, nearly 50% of ARA (precursor of AEA and 2-AG) (64–67) and 90% of oral cannabinoid (68–72) undergo first-pass clearance by liver.

Fifth, loss of FABP1 markedly increased ARA-containing endocannabinoid (AEA, 2-AG) levels in liver (shown herein) and brain (13) of male mice. Despite similar endpoint, however, these increases were likely due to somewhat different mechanisms since FABP1 is not found in brain (11–13,53). For example, FABP1 gene ablation appears to indirectly increase brain AEA and 2-AG levels by: i) increasing plasma ARA availability for uptake in brain which would facilitate AEA and 2-AG synthesis; ii) decreasing expression of several other cytosolic EC binding proteins in brain which would normally facilitate targeting to AEA and 2-AG degradative enzymes (13). Conversely, the data presented herein suggest that FABP1 gene ablation increased AEA and 2-AG levels in liver by: i) directly decreasing cytosolic capacity to bind and/or enhance ARA uptake and intracellular targeting to AEA and 2-AG synthetic pathways; ii) directly binding AEA and 2-AG for targeting to degradative enzymes—the expression of several of which (NAAA, MAGL) was decreased. Furthermore, the impact of FABP1 gene ablation on non-ARA containing EC levels (OEA, PEA, EPEA, 2-OG, 2-PG) in brain differed significantly to that in liver. While loss of

FABP1 increased brain levels of OEA, PEA, 2-OG, and 2-PG (13), FABP1 gene ablation increased liver levels of EPEA and 2-OG while decreasing that of PEA (shown herein) in male mice. While non-ARA containing ECs do not bind CB receptors, they nevertheless enter the nucleus to downregulate PPARα transcription of fatty acid oxidative genes (*Cpt1*) and decrease lipid accumulation—effects opposite to those exhibited by AEA which increases lipid accumulation (51,73–75).

In summary, the data presented herein provide two novel contributions to the endocannabinoid field: i) FABP1 bound ECs, cannabinoids, and inhibitors with high affinity. This suggests that the FABP1 displacement assays developed herein (i.e. direct FABP1 binding of NBD-AEA; displacement of FABP1-bound *cis*-parinaroyl-CoA) may be useful preclinical model for screening cannabinoid agonists/antagonists/inhibitors to be cleared by liver; ii) FABP1 gene ablated mice provide an important physiological pre-clinical model for testing the physiological role(s) of FABP1 in impacting the endocannabinoid system not only in brain but also in liver. This suggests that FABP1 may be a future target for development of novel pharmaceuticals to diminish pain, appetite, and diminish hepatic fat accumulation as in NAFLD, AFLD, and diet-induced obesity (49).

Acknowledgments

We gratefully acknowledge the generosity of ThermoScientific in providing access to the Exactive Orbitrap mass spectrometer and TraceFinder software used for LC/MS herein.

Funding Sources: This work was supported in part by the US Public Health Service/National Institutes of Health Grant R25 OD016574 (S.C., A.B.K. PD) and Merial Veterinary Scholars Program, CVM (S.C., A.B.K. PD).

Abbreviations

ACBP	acyl-CoA binding protein
ACCα	acetyl-CoA carboxylase-α (*Acaca* gene)
ACOX1	acyl CoA oxidase-1 (*Acox1* gene)
ARA	C20:4n-6 arachidonic acid
ACC	acetyl-CoA carboxylase
AEA	N-acylethanolamide (anandamide)
ACOX1	acyl-CoA oxidase 1, palmitoyl (*Acox1* gene)
AFLD	alcoholic fatty liver disease
2-AG	2-arachidonoylglycerol
ANS	1-anilinonaphthalene-8-sulfonic acid
ATGL	adipose triglyceride lipase (*Pnpla2* gene)
CPT1A	carnitine palmitoyltransferase 1A (*Cpt1a* gene)
CB1	cannabinoid receptor-1

CB2	cannabinoid receptor-2
CGI58	comparative gene identification-58 or 1-acylglycerol-3-phosphate O-acyltransferase (*Abhd5* gene)
***cis*-PnCoA**	*cis*-parinaroyl-CoA
DAGLα	diacylglycerol lipase-α
DAGLβ	diacylglycerol lipase-β
DAUDA	11-(dansylamino)-undecanoic acid
DGAT2	diacylglycerol O-acyltransferase 2
DHEA	(n-3 docosahexaenoylethanolamide)
EC	endocannabinoids
ECS	endocannabinoid system
FABP1	liver fatty acid binding protein
FABP3	heart fatty acid binding protein-3
FABP4	adipocyte fatty acid binding protein
FABP5	epidermal fatty acid binding protein
FABP7	brain fatty acid binding protein
FASN	fatty acid synthase (*Fasn* gene)
FATP2, 4, and 5	fatty acid translocase protein-2,4, and 5
GPCR*s	G protein-coupled receptors other than CB1/CB2
GPR119	G protein-coupled receptor 119
HSP70	heat shock protein 70
LC/MS	liquid chromatography/mass spectrometry
LKO	FABP1 gene ablated mouse on C57BL/6NCr background
MAGL	monoacylglycerol lipase
2-MG	2-monoacylglycerol
NAAA	N-acylethanolamide acid amide hydrolase
NAE	N-acylethanolamide
NAFLD	non-alcohol fatty liver disease
NAPE-PLD	N-acyl phosphatidylethanolamine phospholipase D

NBD-AEA	NBD-N-arachidonoylethanolamide or [20-[(7-nitro-2-1,3-benzoxadiazol-4-yl)amino] arachidonoylethanolamide
NBD-stearic acid	12-N-methyl-(7-nitrobenz-2-oxa-1,3-diazo)-aminostearic acid
OEA	oleoylethanolamide
2-OG	2-oleoylglycerol
PEA	palmitoylethanolamide
2-PG	2-palmitoylglycerol
PPARα, -β/δ	peroxisome proliferator-activated receptor alpha or beta/delta (*Ppara* or *b* gene)
SCP2	sterol carrier protein-2
SREBP1c	sterol regulatory element binding protein-1c (encoded by *Srepf1* gene)
WT	wild-type C57BL/6NCr mouse.

References

1. Alswat KA. The role of endocannabinoid system in fatty liver disease and therapeutic potential. Saudi Journal of Gastroenterology. 2015; 19:144–151.
2. Muccioli GG. Endocannabinoid biosynthesis and inactivation, from simple to complex. Drug Discovery Today. 2010; 15:474–483. [PubMed: 20304091]
3. Fowler CJ. Transport of endocannabinoids across plasma membrane and within the cell. FEBS J. 2013; 280:1895–1904. [PubMed: 23441874]
4. Elmes MW, Kaczocha M, Berger WT, Leung KN, Ralph BP, Wang L, Sweeney JM, Miyauchi JT, Tsirka SE, Ojima I, Deutsch DG. Fatty acid binding proteins are intracellular carriers for delta-9-tetrahydrocannabinol (THC) and cannabidiol (CBD). J Biol Chem. 2015; 290:8711–8721. [PubMed: 25666611]
5. Kaczocha LM, Glaser ST, Deutsch DG. Identification of intracellular carriers for the endocannabinoid anandamide. Proc Natl Acad Sci U S A. 2009; 106:6375–6380. [PubMed: 19307565]
6. Kaczocha M, Vivieca S, Sun J, Glaser ST, Deutsch DG. Fatty acid binding proteins transport N-acylethanolamines to nuclear receptors and are targets of endocannabinoid transport inhibitors. J Biol Chem. 2012; 287:3415–3424. [PubMed: 22170058]
7. Berger WT, Ralph BP, Kaczocha M, Sun J, Balius TE, Rizzo RC, Haj-Dahmane S, Ojima I, Deutsch DG. Targeting FABP anandamide transporters--a novel strategy for development of anti-inflammatory and anti-nociceptive drugs. PLoS ONE. 2012; 7:e50968. [PubMed: 23236415]
8. Kaczocha, M. Ph D Thesis. Stony Brook University; 2009. Role of fatty acid binding proteins and FAAH-2 in endocannabinoid uptake and inactivation.
9. Kaczocha M, Rebecchi MJ, Ralph BP, Teng YHG, Berger WT, Galbavy W, Elmes MW, Glaser ST, Wang L, Rizzo RC, Deutsch DG, Ojima I. Inhibition of fatty acid binding protein elevates brain anandamide levels and produces analgesia. PLoS ONE. 2014; 9:e94200. [PubMed: 24705380]
10. Kaczocha M, Glaser ST, Maher T, Clavin B, Hamilton J, O'Rourke J, Rebecchi M, Puopolo M, Owada Y, Thanos PK. Fatty acid binding protein deletion suppresses inflammatory pain through endocannabinoid/N-acylethanolamine-dependent mechanisms. Molecular Pain. 2015; 11:52. [PubMed: 26311517]

11. Myers-Payne S, Fontaine RN, Loeffler AL, Pu L, Rao AM, Kier AB, Wood WG, Schroeder F. Effects of chronic ethanol consumption on sterol transfer protein in mouse brain. J Neurochem. 1996; 66:313–320. [PubMed: 8522969]
12. Avdulov, NA., Chochina, SV., Myers-Payne, S., Hubbell, T., Igbavboa, U., Schroeder, F., Wood, WG. Expression and lipid binding of sterol carrier protein-2 and liver fatty acid binding proteins: differential effects of ethanol in vivo and in vitro. In: Riemersma, RAARKRWaWR., editor. Essential Fatty Acids and Eicosanoids: Invited Papers from the Fourth International Congress. American Oil Chemists Society Press; Champaign, IL: 1998. p. 324-327.
13. Martin G, Chung S, Landrock D, Landrock KK, Huang H, Dangott LJ, Peng X, Kaczocha M, Seeger DR, Murphy EJ, Golovko MY, Kier AB, Schroeder F. FABP1 gene ablation impacts brain endocannabinoid system in male mice. J Neurochem. 2016; :1–16.doi: 10.1111/jnc.13664
14. Atshaves BP, McIntosh AL, Lyuksyutova OI, Zipfel WR, Webb WW, Schroeder F. Liver fatty acid binding protein gene ablation inhibits branched-chain fatty acid metabolism in cultured primary hepatocytes. J Biol Chem. 2004; 279:30954–30965. [PubMed: 15155724]
15. Storey SM, McIntosh AL, Huang H, Martin GG, Landrock KK, Landrock D, Payne HR, Kier AB, Schroeder F. Loss of intracellular lipid binding proteins differentially impacts saturated fatty acid uptake and nuclear targeting in mouse hepatocytes. Am J Physiol Gastrointest and Liver Phys. 2012; 303:G837–G850.
16. Martin GG, Danneberg H, Kumar LS, Atshaves BP, Erol E, Bader M, Schroeder F, Binas B. Decreased liver fatty acid binding capacity and altered liver lipid distribution in mice lacking the liver fatty acid binding protein (L-FABP) gene. J Biol Chem. 2003; 278:21429–21438. [PubMed: 12670956]
17. Murphy EJ, Prows DR, Jefferson JR, Schroeder F. Liver fatty acid binding protein expression in transfected fibroblasts stimulates fatty acid uptake and metabolism. Biochim Biophys Acta. 1996; 1301:191–198. [PubMed: 8664328]
18. Murphy EJ. L-FABP and I-FABP expression increase NBD-stearate uptake and cytoplasmic diffusion in L-cells. Am J Physiol. 1998; 275:G244–G249. [PubMed: 9688651]
19. Prows DR, Murphy EJ, Schroeder F. Intestinal and liver fatty acid binding proteins differentially affect fatty acid uptake and esterification in L-Cells. Lipids. 1995; 30:907–910. [PubMed: 8538377]
20. McIntosh AL, Huang H, Atshaves BP, Wellburg E, Kuklev DV, Smith WL, Kier AB, Schroeder F. Fluorescent n-3 and n-6 very long chain polyunsaturated fatty acids: three photon imaging and metabolism in living cells overexpressing liver fatty acid binding protein. J Biol Chem. 2010; 285:18693–18708. [PubMed: 20382741]
21. Frolov A, Cho TH, Murphy EJ, Schroeder F. Isoforms of rat liver fatty acid binding protein differ in structure and affinity for fatty acids and fatty acyl CoAs. Biochemistry. 1997; 36:6545–6555. [PubMed: 9174372]
22. Huang H, Atshaves BP, Frolov A, Kier AB, Schroeder F. Acyl-coenzyme A binding protein expression alters liver fatty acyl coenzyme A metabolism. Biochemistry. 2005; 44:10282–10297. [PubMed: 16042405]
23. Martin GG, Atshaves BP, Huang H, McIntosh AL, Williams BW, Pai PJ, Russell DH, Kier AB, Schroeder F. Hepatic phenotype of liver fatty acid binding protein (L-FABP) gene ablated mice. Am J Physiol. 2009; 297:G1053–G1065.
24. Chao H, Zhou M, McIntosh A, Schroeder F, Kier AB. Acyl CoA binding protein and cholesterol differentially alter fatty acyl CoA utilization by microsomal acyl CoA: cholesterol transferase. J Lipid Res. 2003; 44:72–83. [PubMed: 12518025]
25. Frolov A, Cho TH, Billheimer JT, Schroeder F. Sterol carrier protein-2, a new fatty acyl coenzyme A-binding protein. J Biol Chem. 1996; 271:31878–31884. [PubMed: 8943231]
26. Schroeder F, Myers-Payne SC, Billheimer JT, Wood WG. Probing the ligand binding sites of fatty acid and sterol carrier proteins: effects of ethanol. Biochemistry. 1995; 34:11919–11927. [PubMed: 7547928]
27. Frolov AA, Schroeder F. Time-resolved fluorescence of intestinal and liver fatty acid binding proteins: Role of fatty acyl CoA and fatty acid. Biochem. 1997; 36:505–517. [PubMed: 9012666]

28. Frolov AA, Schroeder F. Acyl coenzyme A binding protein: conformational sensitivity to long chain fatty acyl-CoA. J Biol Chem. 1998; 273:11049–11055. [PubMed: 9556588]
29. Huang H, McIntosh AL, Martin GG, Landrock K, Landrock D, Gupta S, Atshaves BP, Kier AB, Schroeder F. Structural and functional interaction of fatty acids with human liver fatty acid binding protein (L-FABP) T94A variant. FEBS J. 2014; 281:2266–2283. [PubMed: 24628888]
30. Thumser AE, Voysey JE, Wilton DC. The binding of lysophospholipids to rat liver fatty acid-binding protein and albumin. Biochem J. 1994; 301:801–806. [PubMed: 8053904]
31. Martin GG, Huang H, Atshaves BP, Binas B, Schroeder F. Ablation of the liver fatty acid binding protein gene decreases fatty acyl CoA binding capacity and alters fatty acyl CoA pool distribution in mouse liver. Biochem. 2003; 42:11520–11532. [PubMed: 14516204]
32. Wang L, Liu J, Harvey-White J, Zimmer A, Kunos G. Endocannabinoid signaling via cannabinoid receptor 1 is invovled in ethanol prference and its age-dpendent decline in mice. Proc Natl Acad Sci U S A. 2003; 100:1393–1398. [PubMed: 12538878]
33. Jian W, Edom R, Weng N, Zannikos P, Zhang Z, Wang H. Validation and application of an LC-MS/MS method for quantitation of three fatty acid ethanolamides as biomarkers for fatty acid hydrolase inhibitionin human placenta. J Chrom B. 2010; 878:1687–1699.
34. Schroeder F, Jolly CA, Cho TH, Frolov AA. Fatty acid binding protein isoforms: structure and function. Chem Phys Lipids. 1998; 92:1–25. [PubMed: 9631535]
35. Martin GG, McIntosh AL, Huang H, Gupta S, Atshaves BP, Kier AB, Schroeder F. Human liver fatty acid binding protein (L-FABP) T94A variant alters structure, stability, and interaction with fibrates. Biochemistry. 2013; 52:9347–9357. [PubMed: 24299557]
36. Chuang S, Velkov T, Horne J, Porter CJH, Scanlon MJ. Characterization of the drug binding specificity of rat liver fatty acid binding protein. J Med Chem. 2008; 51:3755–3764. [PubMed: 18533710]
37. Furuhashi M, Tuncman G, Gorgun CZ, Makowski L, Atsumi G, Vallaincourt E, Kono K, Babaev VR, Fazio S, Linton MF, Sulsky R, Robl JA, Parker RA, Hotamisligil GS. Treatment of diabetes and atherosclerosis by inhibiting fatty acid binding protein aP2. Nature. 2008; 447:959–965.
38. McArthur MJ, Atshaves BP, Frolov A, Foxworth WD, Kier AB, Schroeder F. Cellular uptake and intracellular trafficking of long chain fatty acids. J Lipid Res. 1999; 40:1371–1383. [PubMed: 10428973]
39. Hamilton JA. Fatty Acid transport:difficult or easy. J Lipid Res. 1998; 39:467–481. [PubMed: 9548581]
40. Hamilton JA. Fast flip-flop of cholesterl and fatty acids in membranes: implicaitons for membrane transport proteins. Cur Opin Lipidology. 2003; 14:263–271.
41. Kleinfeld AM, Chu P, Romero C. Transport of long-chain native fatty acids across lipid bilayer membranes indicates that transbilayer flip-flop is rate limiting. Biochemistry. 1997; 36:14146–14158. [PubMed: 9369487]
42. Glaser ST, aczocha M, eutsch DG. Anandamide transport: A critical review. Life Sci. 2005; 77:1584–1604. [PubMed: 15979096]
43. Alexander SPH. Therapeutic potential of cannabis-related drugs. Prog in Neuro-Phsychopharm & Biol Psychiatry. 2016; 64:157–166.
44. Frolov A, Miller K, Billheimer JT, Cho TC, Schroeder F. Lipid specificity and location of the sterol carrier protein-2 fatty acid binding site: A fluorescence displacement and energy transfer study. Lipids. 1997; 32:1201–1209. [PubMed: 9397406]
45. Ek BA, Cistola DP, Hamilton JA, Kaduce TL, Spector AA. Fatty acid binding proteins reduced 15-lipoxygenase-induced oxygenation of linoleic acid and arachidonic acid. Biochim Biophys Acta. 1997; 1346:75–85. [PubMed: 9187305]
46. Watkins PA. Very long chain acyl-CoA synthetases. J Biol Chem. 2008; 283:1773–1777. [PubMed: 18024425]
47. Oddi S, Fezza F, Pasquoriello N, et al. Molecular identification of albumin and Hsp70 as cytosolic anandamide binding proteins. Chemistry and Biology. 2009; 16:624–632. [PubMed: 19481477]
48. Regnell SE. Cannabinoid 1 receptor in fatty liver. Hepatol Res. 2013; 43:131–138. [PubMed: 22994399]

49. Schroeder F, McIntosh AL, Martin GG, Huang H, Landrock D, Chung S, Landrock KK, Dangott LJ, Li S, Kaczocha M, Murphy EJ, Atshaves BP, Kier AB. Fatty acid binding protein-1 (FABP1) and the human FABP1 T94A variant: Roles in the endocannabinoid system and dyslipidemias. Lipids. 2016; 51:655–676. [PubMed: 27117865]
50. Osei-Hyiaman D, Liu J, Zhou L, Godlewski G, Harvey-White J, Jeong W, Batkai S, Marsicano G, Lutz B, Buettner C, Kunos G. Hepatic CB1 receptor is required for development of diet-induced steatosis, dyslipidemia, and insulin and leptin resistance in mice. J Clin Inv. 2008; 118:3160–3169.
51. Tam J, Liu J, Mukhopadhyay B, Cinar R, Godlewski G, Kunos G. Endocannabinoids in liver disease. Hepatology. 2011; 53:346–355. [PubMed: 21254182]
52. Atshaves BP, Martin GG, Hostetler HA, McIntosh AL, Kier AB, Schroeder F. Liver fatty acid binding protein (L-FABP) and Dietary Obesity. Journal of Nutritional Biochemisty. 2010; 21:1015–1032.
53. Owada Y, Abdelwahab SA, et al. Altered emotional behavioral responses in mice lacking brain type FABP gene. Eur J Neurosci. 2006; 24:175–187. [PubMed: 16882015]
54. Schroeder, F., Frolov, A., Schoer, J., Gallegos, A., Atshaves, BP., Stolowich, NJ., Scott, AI., Kier, AB. Intracellular sterol binding proteins, cholesterol transport and membrane domains. In: Chang, TY., Freeman, DA., editors. Intracellular Cholesterol Trafficking. Kluwer Academic Publishers; Boston: 1998. p. 213-234.
55. Gossett RE, Frolov AA, Roths JB, Behnke WD, Kier AB, Schroeder F. Acyl Co A binding proteins: multiplicity and function. Lipids. 1996; 31:895–918. [PubMed: 8882970]
56. Gallegos AM, Atshaves BP, Storey SM, Starodub O, Petrescu AD, Huang H, McIntosh A, Martin G, Chao H, Kier AB, Schroeder F. Gene structure, intracellular localization, and functional roles of sterol carrier protein-2. Prog Lipid Res. 2001; 40:498–563. [PubMed: 11591437]
57. Favretto F, Assfalg M, Gallo M, Cicero DO, D'Onofrio M, Molinari H. Ligand binding promiscuity and human liver fatty acid binding protein: structural and dynamic insights from an interaction study with glycocholate and oleate. ChemBioChem. 2013; 14:1807–1819. [PubMed: 23757005]
58. Murphy EJ, Edmondson RD, Russell DH, Colles SM, Schroeder F. Isolation and characterization of two distinct forms of liver fatty acid binding protein from the rat. Biochim Biophys Acta. 1999; 1436:413–425. [PubMed: 9989272]
59. Ockner RK, Manning JA, Kane JP. Fatty acid binding protein. Isolation from rat liver, characterization, and immunochemical quantification. J Biol Chem. 1982; 257:7872–7878. [PubMed: 6806286]
60. DeMarco AC, Patterson PP, Cantrill RC, Horrobin DF. Modification of the fatty acid binding profile of liver fatty acid binding protein (L-FABP). J Nutr Biochem. 1993; 4:515–522.
61. Myers-Payne SC, Hubbell T, Pu L, Schnutgen F, Borchers T, Wood WG, Spener F, Schroeder F. Isolation and characterization of two fatty acid binding proteins from mouse brain. J Neurochem. 1996; 66:1648–1656. [PubMed: 8627322]
62. Pu L, Igbavboa U, Wood WG, Roths JB, Kier AB, Spener F, Schroeder F. Expression of Fatty Acid Binding Proteins Is Altered in Aged Mouse Brain. Molecular and Cellular Biochemistry. 1999; 198:69–78. [PubMed: 10497880]
63. Pu L, Annan RS, Carr SA, Frolov A, Wood WG, Spener F, Schroeder F. Isolation and identification of a native fatty acid binding protein form mouse brain. Lipids. 1999; 34:363–373. [PubMed: 10443969]
64. Mashek DG. Hepatic fatty acid trafficking: multiple forks in the road. Adv Nutr. 2013; 4:697–710. [PubMed: 24228201]
65. Havel RJ, Felts JM, Van Duyne CM. Formation and fate of endogenous triglycerides in blood plasma of rabbits. J Lipid Res. 1962; 3:297–308.
66. Kohout M, Kohoutova B, Heimberg M. The regulaton of hepatic triglyceride metabolism by free fatty acids. J Biol Chem. 1971; 246:5067–5074. [PubMed: 4328243]
67. Zhou L, Vessby B, Nilsson A. Quantitative role of plasma free fatty acids in the supply of arachidonic acid to extrahepatic tissues in rats. J Nutr. 2002; 132:2626–2631. [PubMed: 12221221]

68. Huestis MA. Human cannabinoid pharmacokinetics. Chem Biodivers. 2007; 4:1770–1804. [PubMed: 17712819]
69. Mattes RD, Shaw LM, Edling-Owens J, Engelman K, Elsohly MA. Bypassing the first-pass effect for the therapeutic use of cannabinoids. Pharm Biochem and Behavior. 1993; 44:745–747.
70. Trevaskis NL, Shackleford DM, Charman WN, Edwards GA, et al. Intestinal lymphatic transport enhances the post-prandial oral bioavailability of a novel cannabinoid receptor agonist via avoidance of first-pass metabolism. Pharm Res. 2009; 26:1486–1495. [PubMed: 19280324]
71. Grotenhermen F. Clin Pharmacokinet. 2003; 42:327–360. [PubMed: 12648025]
72. Ashton CH. Pharmacology and effects of cannabis: a brief review. Br J Psychiatry. 2001; 178:101–106. [PubMed: 11157422]
73. Purohit V, Rapaka R, Shurtleff D. Role of cannabinoids in the development of fatty liver (steatosis). AAPS Journal. 2010; 12:233–237. [PubMed: 20204561]
74. Auguet, T., Berlenga, A., Guiu-Jurado, E., et al. Endocannabinoid receptors gene experssion in morbidly obese women with NAFLD; BioMed Res Int. 2014. p. 1-7.dx.doi.org/10.1155/2014/502542
75. Naughton SS, Mathai ML, Hryciw DH, McAinch AJ. Fatty acid modulation of the endocannabinoid system and the effect on food intake and metabolism. Int J Endocrinol ID 361895. 2013:1–11.
76. Martin GG, Atshaves BP, Landrock KK, Landrock D, Schroeder F, Kier AB. Loss of L-FABP, SCP-2/SCP-x, or both Induces Hepatic Lipid Accumulation in Female Mice. Arch Biochem Biophys. 2015; 580:41–49. [PubMed: 26116377]
77. Atshaves BP, McIntosh AL, Payne HR, Mackie J, Kier AB, Schroeder F. Effect of branched-chain fatty acid on lipid dynamics in mice lacking liver fatty acid binding protein gene. Am J Physiol. 2005; 288:C543–C558.
78. Atshaves BP, McIntosh AL, Landrock D, Payne HR, Mackie J, Maeda N, Ball JM, Schroeder F, Kier AB. Effect of SCP-x gene ablation on branched-chain fatty acid metabolism. Am J Physiol. 2007; 292:939–951.
79. Atshaves BP, McIntosh AL, Martin GG, Landrock D, Payne HR, Bhuvanendran S, Landrock K, Lyuksyutova OI, Johnson JD, Macfarlane RD, Kier AB, Schroeder F. Overexpression of sterol carrier protein-2 differentially alters hepatic cholesterol accumulation in cholesterol-fed mice. J Lipid Res. 2009; 50:1429–1447. [PubMed: 19289417]
80. Atshaves BP, Payne HR, McIntosh AL, Tichy SE, Russell D, Kier AB, Schroeder F. Sexually dimorphic metabolism of branched chain lipids in C57BL/6J mice. J Lipid Res. 2004; 45:812–830. [PubMed: 14993239]

Summary Statement

FABP1 is major hepatic endocannabinoid and cannabinoid binding protein.

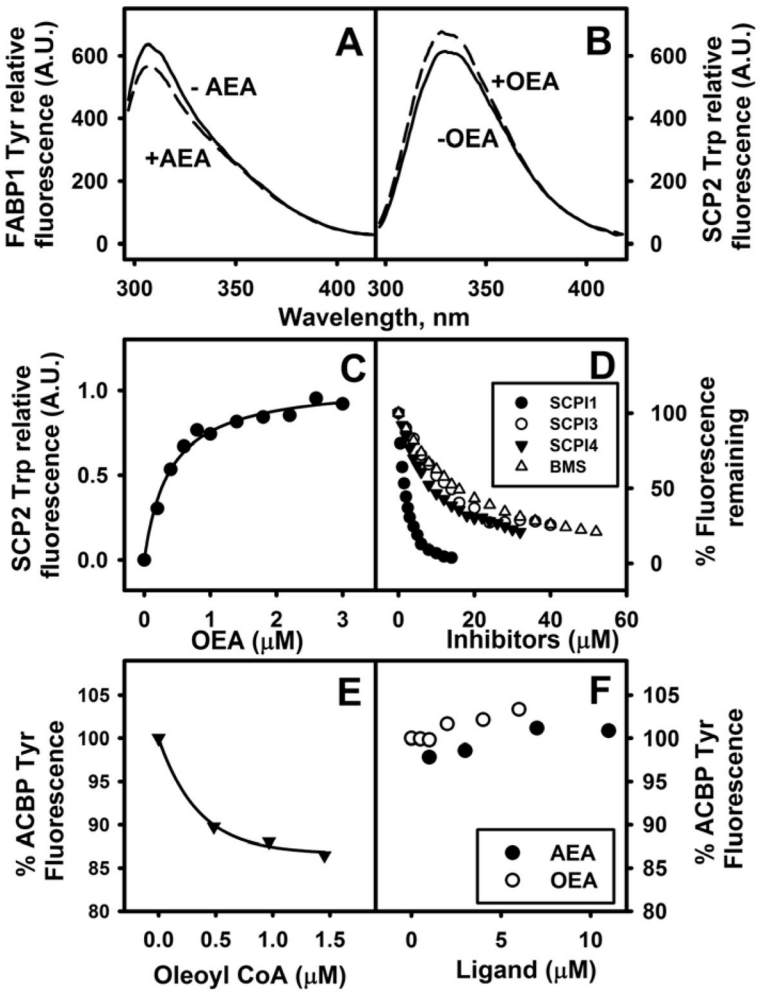

Fig. 1. FABP1 and SCP2 directly bind native endocannabinoids (ECs)

In Panels A–C, direct binding of ECs to FABP1 and SCP2 was determined by impact on FABP1 and SCP2 aromatic amino acid fluorescence emission as described in Methods. (A) FABP1 (500nM) was incubated with (dashed line) or without (solid line) AEA (3μM) and fluorescence emission spectra of FABP1 Tyr determined over the range 295–450 nm, Ex 280 nm. (B) SCP2 (500nM) was incubated with (dashed line) or without (solid line) OEA (1.4 μM) and fluorescence emission spectra of SCP2 Trp determined over the range 295–420 nm, Ex 275 nm. (C) SCP2 (500nM) was titrated with increasing concentration of OEA (0–3 μM) and fluorescence emission maximum of SCP2 Trp monitored with Ex 275nm/Em 330nm. In Panel D, direct binding of inhibitors to SCP2 was determined by displacement of SCP2-bound NBD-stearic acid as described in Methods. SCP2 (500nM) was incubated with NBD-stearate (500nM) and then titrated with increasing concentration of SCP2 inhibitor: SCPI1 (closed black circles), SCPI3 (open circles), SCPI4 (closed black triangles), and FABP inhibitor BMS309403 (open triangles). With increasing amount of inhibitor, NBD-stearate emission decreased (Ex = 490 nm, Em max = 528nm). K_is were calculated from K_d = 0.22 ± 0.03 μM, which was determined by reverse and forward titrations of SCP2 and NBD-stearate, and the EC50 for displacement of NBD-stearate by the respective ligands as

described in Methods. In Panels E–F, direct binding of EC to ACBP was determined by impact on ACBP Tyr/Trp fluorescence emission: (E,F) ACBP (500nM) was incubated with AEA (closed black circles), OEA (open circles), or Oleoyl CoA (solid black triangles) and fluorescence emission spectra of ACBP Tyr/Trp determined over the range 290–450 nm, Ex 274 nm.

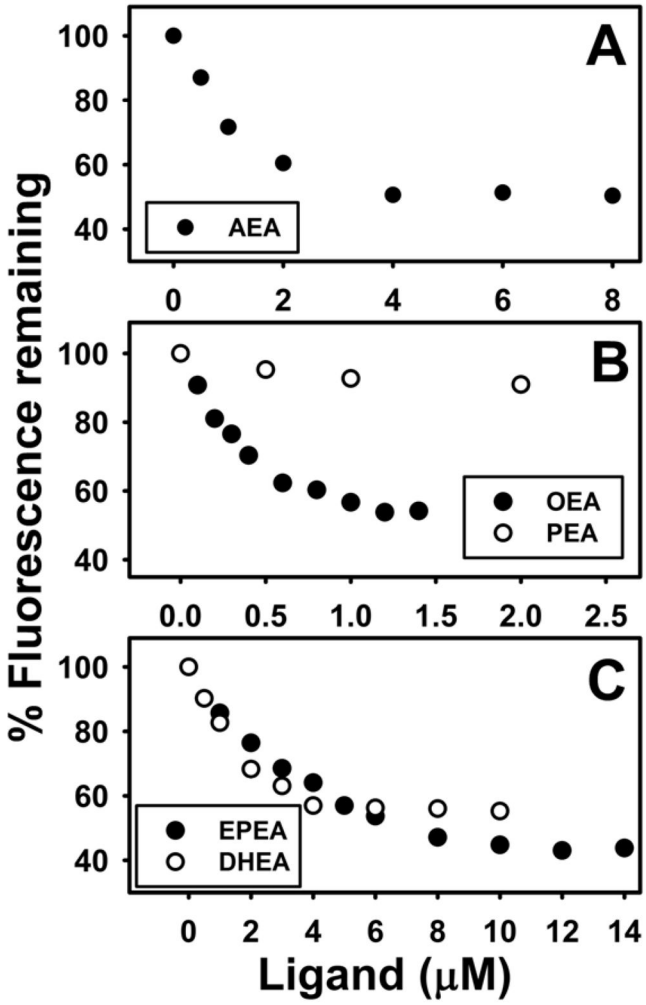

Fig. 2. FABP1 binds N-acylethanolamides (NAEs): displacement of FABP1-bound fluorescent *cis*-parinaroyl-CoA

Displacement assays were performed as in Methods by equilibrating FABP1 (500nM) with *cis*-parinaroyl-CoA (500nM) and then titrating with increasing amount of: (A) AEA (0–8μM); (B) OEA (0–1.5 μM, solid black circles), PEA (0–2μM, open circles); (C). EPEA (0–14μM, solid black circles), DHEA (0–10μM, open circles). As N-acylethanolamide concentration increased, *cis*-parinaroyl-CoA emission (Ex = 304nm, Em max = 420nm) decreased.

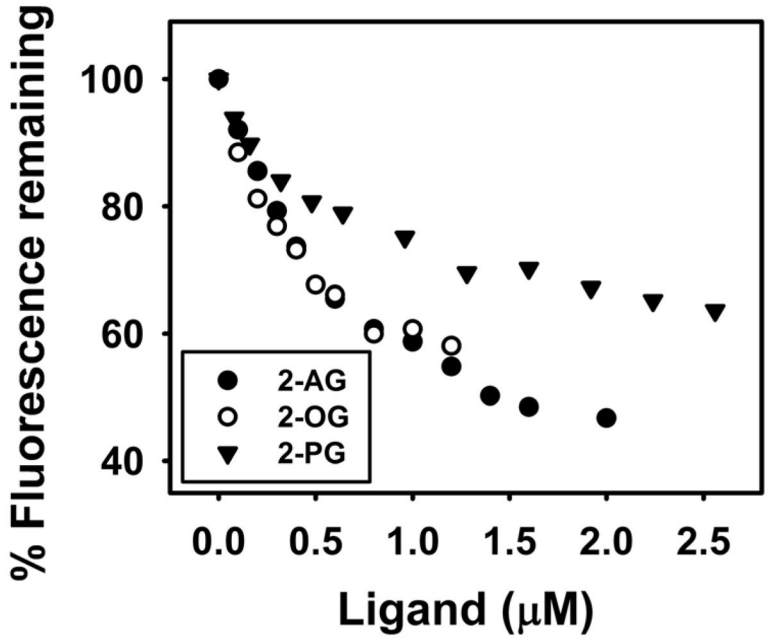

Fig. 3. FABP1 binds 2-monoacylglycerols (2-MGs): displacement of FABP1-bound fluorescent *cis*-parinaroyl-CoA

Displacement assays were performed as in Methods by equilibrating FABP1 (500nM) with *cis*-parinaroyl-CoA (500nM) and then titrating with increasing amount of: 2-AG (0–2μM, solid black circles); 2-OG (0–1.2μM, open circles); or 2-PG (0–2.6μM, solid black triangle). As 2-MG concentration increased, emission of *cis*-parinaroyl-CoA (Ex = 304nm, Em max = 420) decreased.

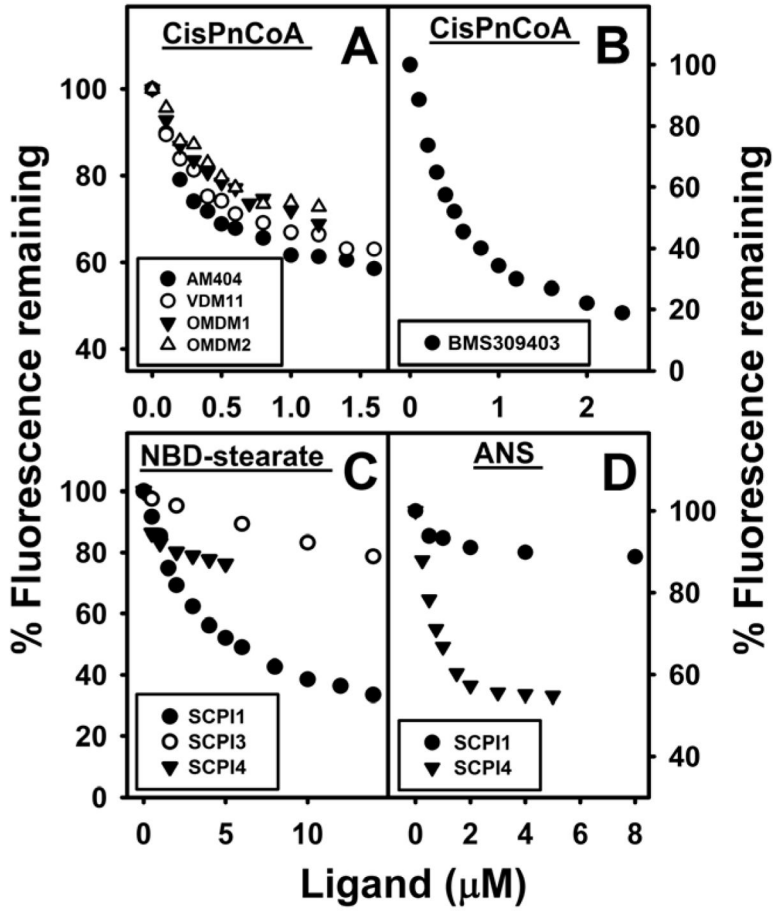

Fig. 4. FABP1 binds inhibitors of N-arachidonoylethanolamide (AEA) uptake, FABPs and SCP2: displacement of FABP1-bound fluorescent *cis*-parinaroyl-CoA and NBD-stearate, or ANS

FABP1-bound *cis*-PnCoA, NBD-stearate, and ANS fluorescence displacement assays were performed as in Methods. Briefly, FABP1 (500nM) was equilibrated with *cis*-parinaroyl-CoA (500nM), NBD-stearate (500nM), or ANS (35μM), and then titrated with increasing amount of AEA uptake inhibitors: (A) AM404 (0–1.6μM, solid black circles), VDM11 (0–1.6μM, open circles), OMDM1 (0–1.2μM, solid black triangles), OMDM2 (0–1.2μM, open triangles); (B) general FABP inhibitor BMS309403 (0–2.4μM, solid black circles); (C,D) SCPI1 (solid black circles); (C) SCPI3 (open circles); and (C,D) SCPI4 (solid black triangles. As inhibitor concentration increased, fluorescence emission of FABP1-bound *cis*-parinaroyl-CoA (Ex = 304nm, Em max = 420), NBD-stearate (Ex = 490nm, Em max = 548nm), and ANS (Ex = 380nm, Em max = 480nm) decreased.

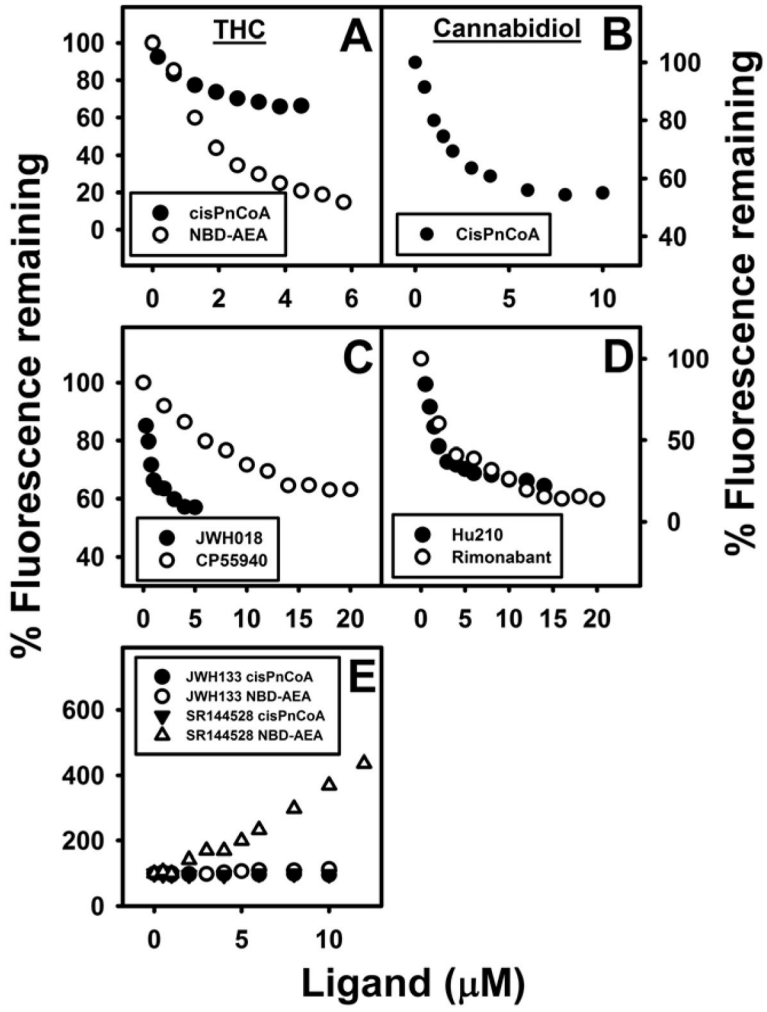

Fig. 5. FABP1 binds phytocannabinoids and synthetic cannabinoids: displacement of FABP1-bound fluorescent *cis*-parinaroyl-CoA and NBD-arachidonoylethanolamide (NBD-AEA)

FABP1-bound *cis*-PnCoA and NBD-AEA fluorescence displacement assays were performed as in Methods. FABP1 (500nM) was equilibrated with *cis*-parinaroyl-CoA (500nM) or NBD-AEA (1μM) and then titrated with increasing amount (0–5μM) of phytocannabinoids: (A) tetrahydrocannabinol (THC) (solid circle, cis-PnCoA displacement; open circle, NBD-AEA displacement); (B) Cannabidiol cis-PnCoA displacement; or synthetic cannabinoids (C) JWH018 cis-PnCoA displacement (solid circle), CP55940 cis-PnCoA displacement (open circles); (D) HU-210 cis-PnCoA displacement (solid circle), Rimonabant cis-PnCoA displacement (open circles); (E) JWH-133 (cis-PnCoA displacement, solid circles; NBD-AEA displacement, open circles); SR-144528 (cis-PnCoA displacement, solid triangles; NBD-AEA displacement, open triangles). As cannabinoid concentration increased, fluorescence emission of *cis*-parinaroyl-CoA emission (Ex = 304nm, Em max = 420) or NBD-AEA (Ex = 490nm, Em = 540nm) were recorded.

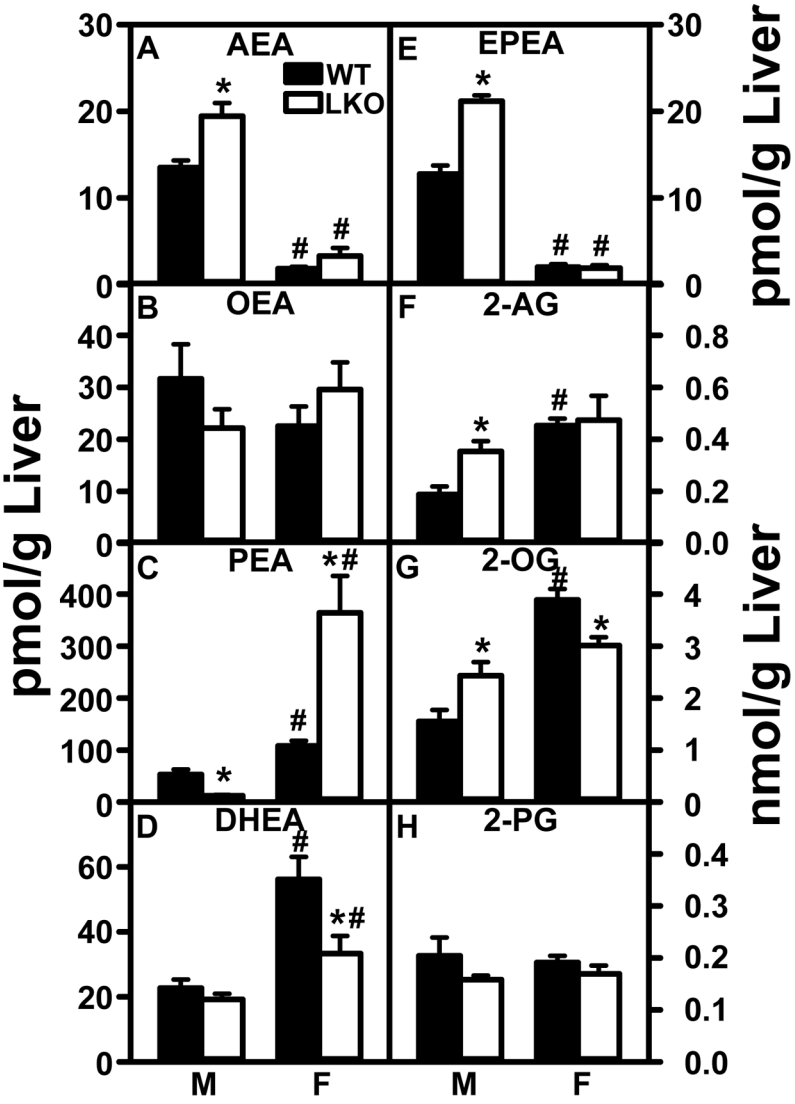

Fig. 6. Impact of FABP1 ablation on liver N-acylethanolamide and 2-monoacylglycerol levels

C57BL/6N male and female WT and FABP1 gene ablated mice (8 wk old) were fed phytol-free, phytoestrogen-free control chow for 3 months, overnight fasted, and livers removed/flash frozen and stored at −80°C. LC-MS analysis to quantitate N-acylethanolamides and 2-monoacylglycerols using deuterated internal standards (Cayman Chemical) was performed as described in Methods to quantitate: (A) arachidonoylethanolamide (AEA); (B) oleoylethanolamide (OEA); (C) palmitoylethanolamide (PEA); (D) docosahexaenoylethanolamide (DHEA), (E) eicosapentaenoylethanolamide (EPEA); (F) 2-arachidonoylmonoglycerol (2-AG); (G) 2-oleoylmonoglycerol (2-OG); H. 2-palmitoylmonoglycerol (2-PG). Values are the mean ± SEM, n=8. *$p<0.05$ for LKO vs WT; $^{\#}p<0.05$ for female vs male of same genotype.

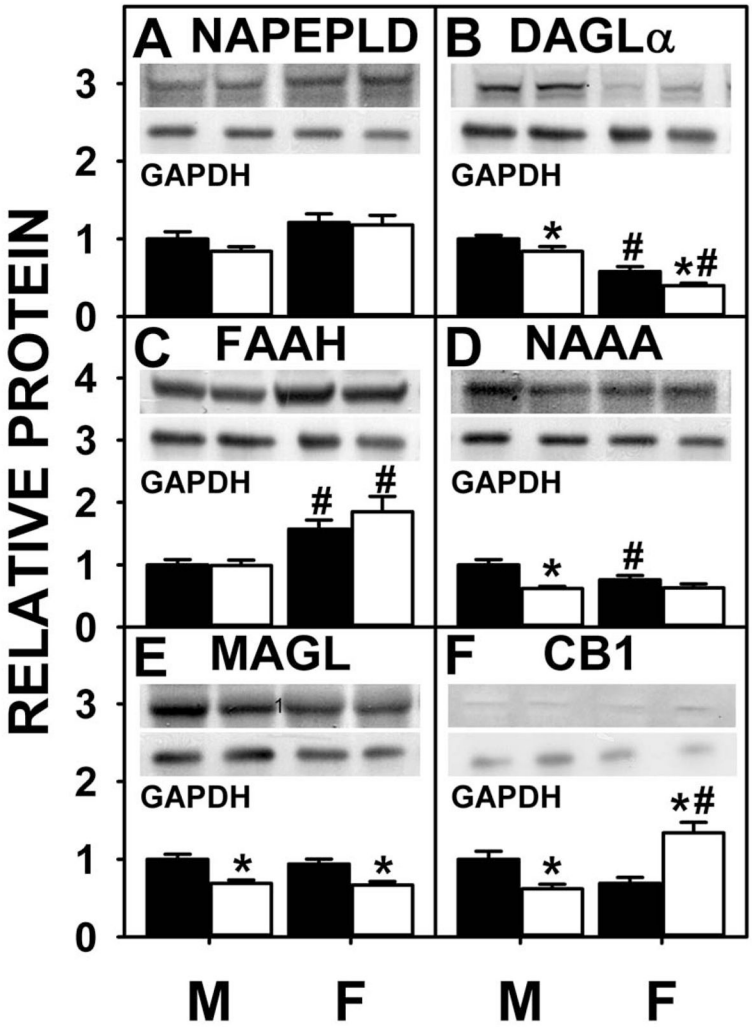

Fig. 7. Effect of FABP1 ablation on protein levels of liver proteins involved in endocannabinoid synthesis, degradation, and action

C57BL/6N male and female WT and FABP1 gene ablate mice (8 wk old) were fed phytol-free, phytoestrogen-free control chow for 3 months, overnight fasted, and livers removed/flash frozen and stored at −80°C. Aliquots of liver homogenate proteins were examined by SDS-PAGE and subsequent western blot analysis as we described (5,76) to determine protein levels of: NAPE-PLD (A), DAGL-α (B), FAAH (C), NAAA (D), MAGL (E), and CB1 (F). Insets show representative western blots of the respective protein (upper blot) and the gel-loading control protein (GAPDH, lower blot). Relative protein was normalized to internal control and WT was set to 1. Values are the mean ± SEM, n=8. *$p<0.05$ for LKO vs WT; $^{\#}p<0.05$ for female vs male of same genotype.

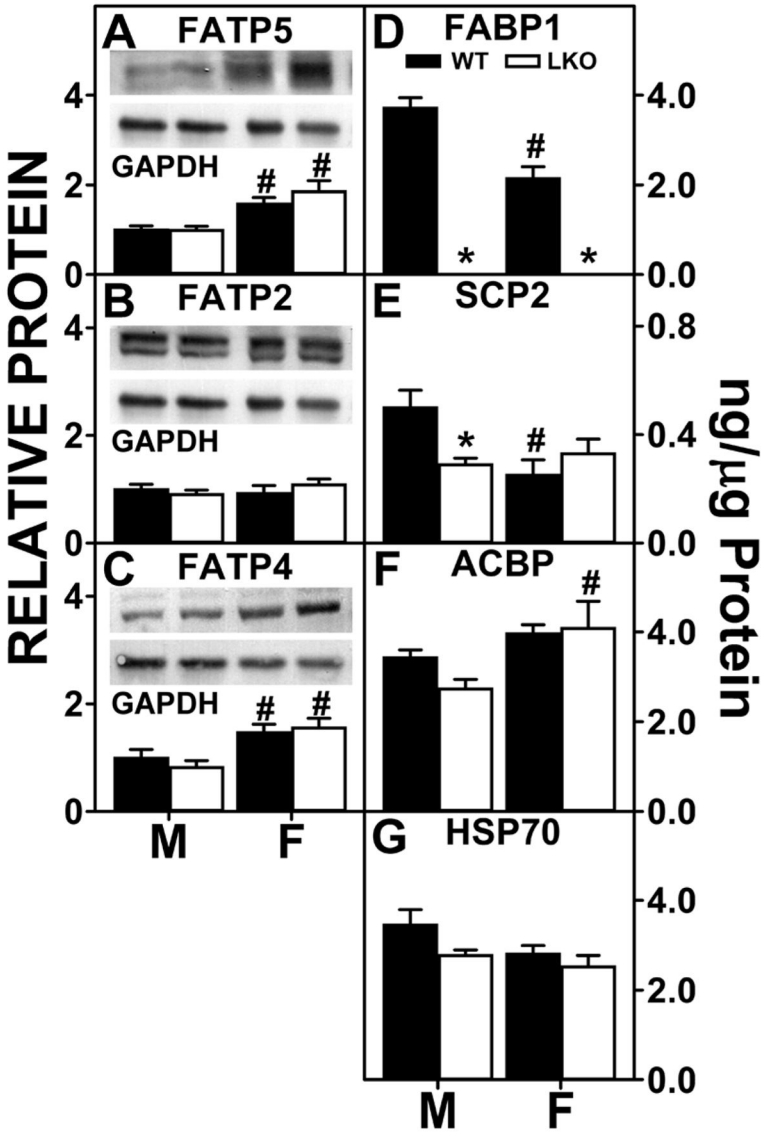

Fig. 8. FABP1 ablation impacts protein levels of liver membrane proteins and cytosolic 'chaperone' proteins involved in fatty acid uptake

All conditions were as in legend to Fig. 7 except that western blot analysis was performed to determine levels of: FATP5 (A), FATP2 (B), and FATP4 (C). Insets show representative western blots of the respective protein (upper blot) and the gel-loading control protein (GAPDH, lower blot). Relative protein was normalized to internal control and WT was set to 1. Mean ± SEM (n=8 different subjects). Quantitative Western blotting to determine protein levels (ng/μg total protein) of FABP1, SCP2, ACBP, and HSP70 was performed by comparison to standard curves of the respective pure recombinant proteins similarly as described for FABP1(77–80). (D) FABP1, (E) SCP2, (F) ACBP, (G) HSP70. Values are the mean ± SEM, n=8. *$p<0.05$ for LKO vs WT; $^{\#}p<0.05$ for female vs male of same genotype.

Table 1

FABP1 has high affinity for N-acyl-ethanolamides, 2-acyl-monoglycerols, and inhibitors

LIGAND	K_i (μM)
ENDOCANNABINOID	
AEA	0.111±0.003[a]
OEA	0.043±0.004[a]
PEA	ND[a,b]
EPEA	0.39±0.03[a]
DHEA	0.163±0.004[a]
2-AG	0.061±0.001[a]
2-OG	0.040±0.003[a]
2-PG	0.070±0.005[a]
AEA UPTAKE INHIBITOR	
AM404	0.029±0.002[a]
VDM11	0.037±0.003[a]
OMDM1	0.040±0.004[a]
OMDM2	0.040±0.005[a]
FABP INHIBITOR	
BMS309403	0.021±0.001(K_{i1}) 0.052±0.001(K_{i2})[a]
SCPI1	0.35±0.05[c]
SCPI3	0.90±0.10[c]
SCPI4	0.033±0.002[d]

K_is were determined as described in Methods from displacement of FABP1-bound fluorescent ligands,

[a] *cis*-parinaroyl-CoA,

[b] NBD-AEA,

[c] NBD-stearic acid, and

[d] ANS.

ND = no significant displacement. Values are the mean ± SEM, n=5.

Table 2

FABP1 has high affinity for phytocannabinoids and some synthetic cannabinoids

LIGAND	Ki (μM)
PHYTOCANNABINOID	
THC	1.0±0.2[b]
Cannabidiol	0.167±0.009[a]
SYNTHETIC CANNABINOID	
HU-210	0.85[b]
JWH 018	0.058±0.005[a]
Rimonabant	2.0±0.4[b]
JWH-133	ND[a,b]
SR-144528	ND[a,b]
CP55,940	0.99±0.07[a]

K_is were determined as described in Methods from displacement of FABP1-bound fluorescent ligands,

[a] *cis*-parinaroyl-CoA and

[b] NBD-AEA.

ND = no significant displacement. Values are the mean ± SEM, n=5.

Table 3

Effect of sex and FABP1 gene ablation (LKO) on transcription of genes encoding liver nuclear receptors and proteins involved in downstream effects of ECs.

	MALE		FEMALE	
mRNA	**WT**	**LKO**	**WT**	**LKO**
Ppara	1.0±0.007	0.91±0.05	1.00±0.07	1.30±0.08 *#
Pparb	1.0±0.004	0.86±0.08	1.17±0.07#	1.33±0.09#
Cpt1a	1.0±0.007	1.12±0.05*	0.71±0.04#	0.63±0.03#
Acox1	1.0±0.027	0.72±0.06*	0.50±0.03#	0.43±0.02#
Srebf1	1.0±0.010	1.23±0.09	1.14±0.08	2.27±0.27 *#
Acaca	1.0±0.011	0.73±0.10*	1.10±0.05	1.2±0.16#
Fasn	1.0±0.010	2.44±0.56*	1.48±0.20	2.46±0.46*
Pnpla2	1.0±0.010	1.03±0.06	1.05±0.06	1.54±0.17 *#
Abhd5	1.0±0.008	1.20±0.10	1.53±0.11#	1.52±0.09#

All conditions were as described in legend to Fig. 7 except that QrtPCR was performed to determine mouse mRNA levels for hepatic nuclear receptors (*Ppara, Pparb, Srebf1)* and target genes in fatty acid metabolism (*Cpt1a, Acox1, Acaca, Fasn, Pnpla2, Abhd5*) similarly as for other mRNAs in brain (13). mRNA levels were normalized to an internal control (18S RNA). Mean ± SEM (n=6–8),

* $p<0.05$ for LKO vs WT;

# $p<0.05$ for female vs male of the same genotype.